



HAL
open science

The chemistry of hyperalkaline springs in serpentinizing environments: 1. the composition of free gases in New Caledonia compared to other springs worldwide

Christophe Monnin, Marianne Quemeneur, Roy Price, Julie Jeanpert, Pierre Maurizot, Cédric Boulart, Jean-Pierre Donval, Bernard Pelletier

► To cite this version:

Christophe Monnin, Marianne Quemeneur, Roy Price, Julie Jeanpert, Pierre Maurizot, et al.. The chemistry of hyperalkaline springs in serpentinizing environments: 1. the composition of free gases in New Caledonia compared to other springs worldwide. *Journal of Geophysical Research: Biogeosciences*, In press, 9 (126), pp.e2021JG006243. 10.1029/2021JG006243 . hal-03242378

HAL Id: hal-03242378

<https://hal.science/hal-03242378>

Submitted on 31 May 2021

HAL is a multi-disciplinary open access archive for the deposit and dissemination of scientific research documents, whether they are published or not. The documents may come from teaching and research institutions in France or abroad, or from public or private research centers.

L'archive ouverte pluridisciplinaire **HAL**, est destinée au dépôt et à la diffusion de documents scientifiques de niveau recherche, publiés ou non, émanant des établissements d'enseignement et de recherche français ou étrangers, des laboratoires publics ou privés.

1
2 **The chemistry of hyperalkaline springs in serpentinizing environments: 1. the**
3 **composition of free gases in New Caledonia compared to other springs worldwide.**
4

5
6 Christophe Monnin^{1*}, Marianne Quéméneur², Roy Price³, Julie Jeanpert⁴, Pierre Maurizot⁴, Cédric Boulart⁵,
7 Jean-Pierre Donval⁶, Bernard Pelletier⁷
8

9 ¹ Géosciences Environnement Toulouse, (CNRS/UPS/IRD/CNES), 14 Avenue E Belin, 31400 Toulouse, France.

10 ² Aix Marseille Univ., Université de Toulon, CNRS, IRD, MIO, Marseille, France.

11 ³ School of Marine and Atmospheric Sciences, Stony Brook, NY, USA.

12 ⁴ DIMENC (Direction de l'Industrie, des Mines et de l'Energie), Nouméa, Nouvelle-Calédonie

13 ⁵ AD2M UMR 7144 (CNRS, Sorbonne Université), Station Biologique de Roscoff, Place Georges Tessier,
14 29680 Roscoff, France

15 ⁶ IFREMER, Unité Géosciences Marines/Laboratoire Cycles Géochimiques, ZI Pointe du Diable. CS 10070.
16 29280 Plouzané, France

17 ⁷ Géoazur (UCA, IRD, CNRS, OCA), Centre IRD de Nouméa, BP A5, Nouméa, Nouvelle-Calédonie.

18
19 Corresponding author: Christophe Monnin (mailto: Christophe.monnin@get.omp.eu)
20
21
22

23 **Key Points:**

- 24 • Hyperalkaline spring waters are anoxic. An elevated high O₂ content in free gases results from air
25 contamination.
- 26 • The relationship between H₂ and CH₄ contents of free gases is consistent with the conversion of fully
27 oxidized carbon (CO₂).
- 28 • The H₂-CH₄ relation is consistent with a Sabatier reaction in the gas or a methane production by
29 hydrogenotrophic methanogens in the water.
30

31
32
33
34
35
36
37
38
39
40
41
42
43
44
45
46
47
48
49
50
51
52

Abstract

Serpentinization is a natural process that transforms ferromagnesian minerals such as olivine into serpentine and that produces waters at very high pH and gases enriched in methane (CH₄) and hydrogen (H₂). We report the composition of gases venting at two springs (Bain des Japonais and Rivière des Kaoris) of the serpentinizing environment of the Prony Bay (New Caledonia) collected eight times between 2011 and 2014, along with in situ measurements (temperature, pH, oxydo-reduction potential, dissolved oxygen content) of on-land alkaline springs of the Southern New Caledonia ophiolite. Venting gases are mainly composed of H₂, CH₄ and N₂ and their composition has slightly varied during the 4-year field survey. An elevated oxygen (O₂) content in a high-pH water sample is due to air uptake during surface flow. O₂-corrected gas compositions along with those published for gas data obtained at similar serpentinizing environments (Italy, Turkey, Philippines, Oman) show that the H₂ and CH₄ concentrations display a linear correlation with a slope close to the value corresponding to the CH₄ production from carbon dioxide rather from a less oxidized carbon such as carbon monoxide. Although these data are consistent with the stoichiometry of the Sabatier reaction, as such in the gas phase, it is also possible that microbial hydrogenotrophic methanogenesis takes place in the aqueous phase followed by degassing. A diagram is proposed that outlines the partitioning of H₂ and CH₄ between the gaseous and aqueous phases and the need to consider a two-phase flow in the hydrology of these hyperalkaline environments.

53 Plain Language Summary

54 Serpentinization is a natural process that transforms ferromagnesian minerals such as olivine into
55 serpentine. This process is accompanied by the formation of high-pH water, hydrogen and methane.
56 This forms a unique ecological niche for microorganisms adapted to extreme pH and/or involved in
57 the hydrogen and/or methane cycles. There is an ongoing debate on the mechanisms at play and on the
58 contribution of abiotic versus biogenic reactions. An analysis of the composition of free gases
59 collected in hyperalkaline springs of New Caledonia combined with literature values for similar sites
60 worldwide shows that the formation of methane follows the stoichiometry of a Sabatier-type reaction
61 involving fully oxidized carbon (CO₂) and not carbon monoxide (CO) as required by a Fischer-
62 Tropsch-Type process. Although it could be concluded that methane production occurs in the gas
63 phase, and as such would be abiotic, it does not rule out the possibility that the relationship between
64 gaseous hydrogen and methane is due to methane production and hydrogen consumption by
65 microorganisms in the aqueous phase followed by degassing.

66

67 1 Introduction

68
69 Natural environments with waters at pH above 11 have received considerable attention in the
70 last decades due to the wide range of scientific questions that they relate to : abiotic formation of
71 hydrocarbons (e.g. [*Etiopie and Sherwood Lollar, 2013; Price et al., 2017; Sissmann et al., 2019*],
72 origin of life and deep subsurface biosphere (e.g., [*Menez et al., 2012; Schrenk et al., 2013*], alteration
73 of the oceanic crust (e.g. [*Debret et al., 2019; Fryer et al., 2020; Ligi et al., 2013*], natural formation
74 of hydrogen as an energy source (e.g. [*Truche et al., 2020*], geological storage of CO₂ [*Kelemen and*
75 *Matter, 2008; Kelemen et al., 2011*], the analogy with planetary surfaces like Mars or Europe [*Holm et*
76 *al., 2015; Szponar et al., 2012*], energy and matter fluxes between geochemical reservoirs [*Plank and*
77 *Manning, 2019*].

78 Sites of discharge of such very high pH waters are found on land in Oman [*Chavagnac et al.,*
79 *2013b; Miller et al., 2016; Paukert et al., 2012; Stanger, 1985*], in Northern Italy; [*Boschetti and*
80 *Toscani, 2008; Chavagnac et al., 2013b; Cipolli et al., 2004*], in Cyprus [*Neal and Shand, 2002*], in
81 the Philippines [*Cardace et al., 2015*], in California [*Boschetti et al., 2017; Morrill et al., 2013*], in
82 Ontario [*Sader et al., 2007*], in Newfoundland [*Szponar et al., 2012*], in Portugal [*Marques et al.,*
83 *2008*], in Greece [*D'Alessandro et al., 2018a*], in Turkey [*Meyer-Dombard et al., 2015; Yuce et al.,*
84 *2014*], in Jordan [*Khoury et al., 1992*], in New Caledonia [*Monnin et al., 2014*] and in Spain
85 [*Giampouras et al., 2019*]. Such hyperalkaline waters are also found underwater in the ocean, at the
86 Lost City Hydrothermal Field on the Atlantis massif off the Mid-Atlantic ridge [*Kelley et al., 2001;*
87 *Kelley et al., 2005*] and in the mud volcanoes of the Marianna forearc [*Fryer et al., 1989; Fryer et al.,*
88 *2018; Mottl et al., 2004*]. The Maqarin site in Jordan is a peculiar case where the natural combustion
89 of bituminous marls and the alteration of the rocks created by a phenomenon that has been called
90 pyrometamorphism lead to the formation of extremely alkaline water, with pH value up to 12.5
91 [*Alexander et al., 1992; Khoury et al., 1992*]. Apart from the Maqarin site, these hyperalkaline waters
92 originate from the serpentinization of ultramafic rocks that can be found on land in ophiolites (e.g.
93 Oman, Liguria, etc.), in an ultramafic complex created by continental collision such as Cabeço de Vide
94 in Portugal [*Marques et al., 2008; Marques et al., 2018*], at the seafloor where plate tectonics has

95 exposed ultramafic rocks to alteration, such as at the Lost City site (Northern Atlantic), or at the
96 decollement zone of the subducting plate in the case of the Marianna forearc mud volcanoes [*Mottl et*
97 *al.*, 2004]. The discharge of these waters is focused and occurs at springs where they lead to the
98 formation of carbonate concretions, in the form of tuffs in Oman [*Chavagnac et al.*, 2013a] or
99 submarine pinnacles at Lost City [*Kelley et al.*, 2005] and in the Prony Bay in New Caledonia [*Launay*
100 *and Fontes*, 1985; *Monnin et al.*, 2014; *Pelletier et al.*, 2006].

101 While the discharge zones (springs) are easily recognized in the field, the recharge of these
102 hydrological systems is poorly or not at all characterized. The geographic extension of a given
103 hydrothermal system, the characterization of the inflowing water, its residence time and the role of the
104 composition of the geological formation (its lithology, its physical and thermal structure) are general
105 questions on any hydrological system. They are rarely documented for hyperalkaline hydrothermal
106 systems [*Christofi et al.*, 2020; *Dewandel et al.*, 2005; *Lods et al.*, 2020; *Marques et al.*, 2018]. A
107 classification of high-pH springs based on the location of the output (marine or continental) and on the
108 origin of the circulating fluid based on the salinity of the spring waters has been proposed [*Monnin et*
109 *al.*, 2014]. Thus, a first category is defined by the fresh high-pH spring waters found in continental
110 environments like in Oman, Liguria, Portugal, Philippines, Greece, and Turkey. The second main
111 category contains hyperalkaline waters with salinities similar to that of seawater discharging at springs
112 located in the marine environment, the Lost City site being the archetype of this category [*Kelley et*
113 *al.*, 2001; *Kelley et al.*, 2005; *Seyfried Jr et al.*, 2015]. This is also the case of the Marianna mud
114 volcanoes, where the high-pH waters have seawater-like salinities, but a very complex geological
115 history linked to their origin in the dehydration of the subducting Pacific plate in the Marianna
116 subduction zone [*Hulme et al.*, 2010; *Mottl et al.*, 2004]. In nearly every case, the inflowing water
117 (recharge) of these hyperalkaline hydrothermal systems is continental (meteoric, runoff) water (low
118 salinity) for systems fully located on continents and seawater for fully marine environments.

119 Two hyperalkaline hydrothermal systems do not fit in this classification. The Aqua de Ney
120 spring is located inland about 200 km from the Northern California Coast. Its water (pH \approx 12) has a
121 salinity similar to that of seawater and is a case of a high-pH saline water discharging in a continental
122 environment [*Blank et al.*, 2017; *Feth et al.*, 1961]. It has been proposed that it originates from the

123 dehydration of the Pacific plate subducting below the American continent [Boschetti *et al.*, 2017]. The
124 other system that does not fit in the classification is in Prony Bay (southern lagoon of New Caledonia)
125 where alkaline springs located in the lagoon discharge fresh waters into the marine environment
126 [Monnin *et al.*, 2014].

127 Globally, these hyperalkaline waters contain elevated concentrations of methane and hydrogen
128 [Etioppe and Whiticar, 2019]. Gas venting is commonly observed but not at every location, while
129 dissolved gases have been analyzed in numerous hyperalkaline springs (see the review of [Etioppe and
130 Whiticar, 2019]. Gas bubbles have been sampled in Oman [Boulart *et al.*, 2013; Vacquand *et al.*,
131 2018], in the Voltri ophiolite in Liguria (Northern Italy) [Boschetti *et al.*, 2013; Boulart *et al.*, 2013;
132 Etioppe and Whiticar, 2019], at several locations in the Philippines [Abrajano *et al.*, 1988; Vacquand *et*
133 *al.*, 2018] and in Turkey [D'Alessandro *et al.*, 2018b; Vacquand *et al.*, 2018] and in New Caledonia
134 [Vacquand *et al.*, 2018]. The gases are mainly composed of dihydrogen (H₂), dinitrogen (N₂) and
135 methane (CH₄), with trace amounts of higher alkanes, carbon dioxide and monoxide and helium.
136 Oxygen is not always measured or reported. It can be found in noticeable concentrations, for example
137 up to 15% for one of the samples of the Kisecek spring in the Kizildag ophiolite in Turkey
138 [D'Alessandro *et al.*, 2018b] or the Zambales springs in the Philippines [Abrajano *et al.*, 1988]).

139 The Prony Bay hydrothermal field (PBHF), that has been studied during the HYDROPRONY
140 cruise in 2011 [Pelletier *et al.*, 2011], comprises several underwater springs in the Prony Bay, with the
141 Aiguille de Prony being the most prominent, and two costal main sites at the northernmost part of the
142 Prony Bay, the Bain des Japonais, a spring that is uncovered at low tide and the Bain des Kaoris that is
143 located above the water level [Monnin *et al.*, 2014]. A number of other springs and seepages of high
144 pH waters are known inland from the coast (Grande Terre) many 10s of kilometers north from Prony
145 Bay ([Maurizot *et al.*, 2020]; Fig. 1). We here present in situ measurements of pH, oxidation-reduction
146 potential (ORP), dissolved oxygen and temperature of these on-land spring waters, along with the
147 compositions of free gases collected at the Bain des Japonais and at the Kaoris springs during a survey
148 carried out between 2011 and 2014.

149 The oxic/anoxic characteristic of the high pH waters has been determined from in situ
150 measurements of the oxygen content directly at the springs, but also from the gas chromatography

151 analysis of the free gases. We address the question of air contamination of the samples and propose a
152 way to correct it. These new data are then compared to sites of alkaline springs in other countries
153 where gas venting is observed. This allows to address the question of the stoichiometry of methane
154 production and hydrogen consumption and therefore the nature of the carbon pool in low temperature
155 serpentinizing environments.

156

157 2 Location and geological setting of the springs

158

159 2.1 The springs of the Prony Bay

160

161

162 The Prony Bay springs have been previously described ([*Monnin et al.*, 2014] and references
163 therein). The Kaoris spring is located above the sea level at the northeastern end of the Bay along the
164 Kaoris River. The Bain des Japonais, which is submerged at high tide, is located on the Baie du
165 Carénage, at the northwestern end of the larger Prony bay [*Monnin et al.*, 2014]. These two sites, 2.2
166 km apart, are easily accessed using a shallow-draft boat. They have been visited several times between
167 2011 and 2014 (Table S2).

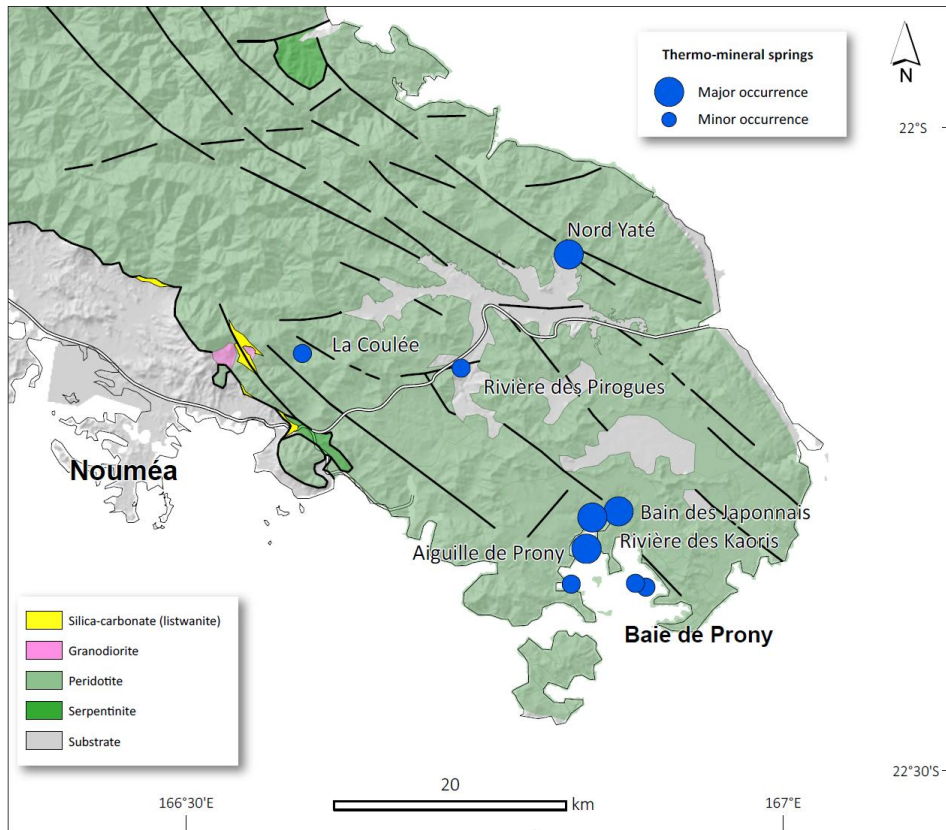
168

169 2.2 On-land springs

170

171 The spring north of the Yaté Lake (called Nord Yaté) has been visited only once on August 8,
172 2013, while the other on-land springs were sampled during the 2014 fall (Nov. 17 to Dec. 15) (Fig. 1).

173



174

175 *Figure 1 – Location of the high pH springs in southern New Caledonia (after [Maurizot et al.,*
 176 *2020]).*

177

178 The spring “La Coulée” is located in the outskirts of Nouméa in the valley of the river “La
 179 Coulée” and is easily accessed. The main water outlet is about two meters above the river bed in a
 180 shallow (about 10-cm deep) pool (Fig. 2). The pools below are fed by water overflowing from the
 181 upper pool. Very intermittent gas bubbling has been observed in the upper pool, but no sample could
 182 be taken because of the very slow discharge (a bubble every 10 mn or so).

183

184 The spring “Rivière des Pirogues” is a little bit further away and can be accessed by dirt roads.
 185 The high pH water outlet is a seepage located within the bed of a tributary of the Pirogues River in
 186 fractured rocks above a large (about 30 m wide) water pool formed at the junction with the Pirogues
 187 river. Bubbling in this pool has been observed about two meters from the rocky bank, but again no
 188 sample could be taken. This spring does not build carbonate pools like the spring “La Coulée” (Fig.
 S1).

189 The spring of the Montagne des Sources (also named Rivière du Rocher) is located in a reserve.
190 The access is totally restricted because this is where the city of Nouméa is getting its water supply
191 from (Fig. S1). A strenuous 5-hour hike in the river bed is required to get to the spring. The spring is a
192 30-m long spectacular suite of large pools located right above the river bed and below a forest (Figure
193 S1). These pools are about 1.5 m in diameter and about 1.5 m deep for the deepest one. Water flows at
194 a high rate through an outlet situated in the middle of the wall of the structure. The pools contain
195 varying amounts of branches and leaves from the trees above. Sampling and observations have been
196 difficult and less extensive than anticipated because of the very bad weather and heavy rain on the day
197 of our visit (Dec. 3, 2014).

198 The spring on the Northern side of the Yaté Lake cannot be reached by land. Water samples
199 were collected during a visit to the spring by helicopter on August 8, 2013, therefore with limited time
200 on the site. Similarly to the Coulée spring, it is located right above the river bed (Fig. S1). The high-
201 pH water builds up small terraces that are common characteristics of these peculiar springs, as can be
202 observed for example at La Coulée spring (Fig. 2), in Oman and Liguria [*Chavagnac et al.*, 2013a;
203 *Chavagnac et al.*, 2013b] or in California at the Cedars spring [*Suzuki et al.*, 2013].

204 Although they have been included in previous studies of New Caledonia alkaline springs [*Cox*
205 *et al.*, 1982; *Deville and Prinzhofer*, 2016; *Vacquand et al.*, 2018], the springs of the Canala area are
206 somewhat different than those further South. The geological substratum is different and the pH (≈ 9)
207 of its waters is lower than that at the other studied sites [*Cox et al.*, 1982; *Maurizot et al.*, 2020;
208 *Quéméneur et al.*, 2021].

209

210 3 Sampling procedures, in situ measurements and analytical methods

211

212 3.1 Free gas sampling procedure and in situ measurements: pH, oxidation-reduction 213 potential, temperature and dissolved oxygen

214

215 Gas samples were collected in 10-ml glass vials by the water displacement technique. It consists
216 in filling the vial with spring water and immersing it upside down in the spring above the gas bubbles.
217 The captured bubbles displace the water from the vial which is then closed with a rubber stopper when

218 there is no water left (then sealed with an aluminum cap). It was noticed that an air bubble can be
219 trapped in the rubber stopper, leading to air contamination. Even if great care is taken, air uptake
220 during sampling is not totally unavoidable. For example, several gas compositions reported by [Neal
221 and Stanger, 1983] and [Sano *et al.*, 1993] for Oman show that almost pure air has been sampled.

222 The samples were kept at 4°C in the laboratories in Nouméa (IRD) and in Marseille (MIO).
223 They were kept at room temperature (i.e. plane cargo bays and lockers) while travelling between New
224 Caledonia and metropolitan France (i.e. for about 30 hours).

225 Temperature, pH, oxidation-reduction potential (ORP) and the dissolved oxygen content were
226 measured directly in the springs with the appropriate probes using a using a WTW Multi 3420®
227 Multimeter that allows recording the measurements over a time period with a fixed step (Fig. S2).
228 Temperature and pH were measured during all the campaigns using a SenTix 940® pH electrode in
229 which a thermocouple allows temperature to be measured. ORP (Oxidation-Reduction Potential in
230 reference to the Ag/AgCl standard) and dissolved oxygen were measured only in 2014 after the
231 acquisition of the appropriate probes (SensoLyt ORP 900-P® for the redox potential and FDO 925®
232 for dissolved oxygen).

233

234 3.2 Gas analyses

235

236 The gas analyses (dissolved and gaseous) were carried out in three different laboratories: MIO
237 (Mediterranean Institute of Oceanography) in Marseille (France), at the Laboratoire des Cycles
238 Géochimiques et ressources (LCG) IFREMER Brest (France) and at the NASA Ames Research
239 Center (Moffett Field, California).

240 At MIO (Marseille) the gas composition was determined using a Shimadzu GC 8A gas
241 chromatograph equipped with a thermal conductivity detector (GC/TCD) and a concentric column
242 CTR1 (Alltech, USA). Argon was used as carrier gas at a flow rate of 60 mL/min; temperature of the
243 injector and the detector was fixed at 150°C. All analyses were run in duplicate.

244 At in the NASA Ames Research Center, The concentrations of free gases were analyzed by a
245 Shimadzu GC 8A gas chromatograph equipped with a thermal conductivity detector (GC/TCD) and

246 two columns (Alltech, USA). Operating conditions for H₂, O₂, CH₄, and CO₂ analyses are as follows:
247 the carrier gas is nitrogen at a pressure of 100 kPa; temperature of the column is fixed at 150°C and
248 that of the injector and the detector is fixed at 200°C. N₂ was determined by difference based on
249 previous estimates [Monnin *et al.*, 2014].

250 At IFREMER Brest, two analytical devices have been used: a gas chromatograph µGC R3000
251 from SRA equipped with three analytical modules to determine hydrogen, oxygen, nitrogen, methane
252 to hexane and carbon dioxide concentrations, and a Agilent 7890A gas chromatograph equipped with
253 a 32 m, 0.32mm Porapak Q column and a triple detection system (TCD-FID-mass detector) to analyze
254 hydrocarbons at low concentrations. The TCD and FID are used for quantitative analysis while the
255 mass spectrometer is used for the purpose of verification of the compounds or identification of
256 unknown compounds against the NIST05 library. The injection and calibration were performed as
257 described by [Donval *et al.*, 2020].

258 The data and the laboratories where the analyses have been made are reported in Table S2.

259 4 Results

260

261 4.1 In situ measurements: temperature, pH, ORP and dissolved oxygen

262

263 4.1.1 Temperature and pH

264

265 The in-situ parameters (Table S1) were recorded during 30 mn at the springs of La Coulée and
266 Pirogues. Dissolved oxygen and ORP required an equilibration time of a few minutes (Fig. S2). The
267 water temperatures at all the on-land springs are between 26 and 32°C, similar to that for the Kaoris
268 (32°C) but a little bit lower than those for the Bain des Japonais (38°). At La Coulée, the water
269 temperature measured in the upper pool is 27°, lower than the air temperature which was 30° or even
270 higher on the days of sampling.

271 pH is constant at Pirogues at a value of 10.88 but varies over 0.2 pH units at La Coulée between
272 10.81 and 11.05 (Table S1). There is a correlation between temperature and pH at La Coulée in the
273 upper pool (Fig. S2). The temperature variation can be due to a convection effect of the thin water

274 layer. Indeed, the discharging water temperature is between about 27°C while the air temperature on
 275 the days of measurements were over 30°C.

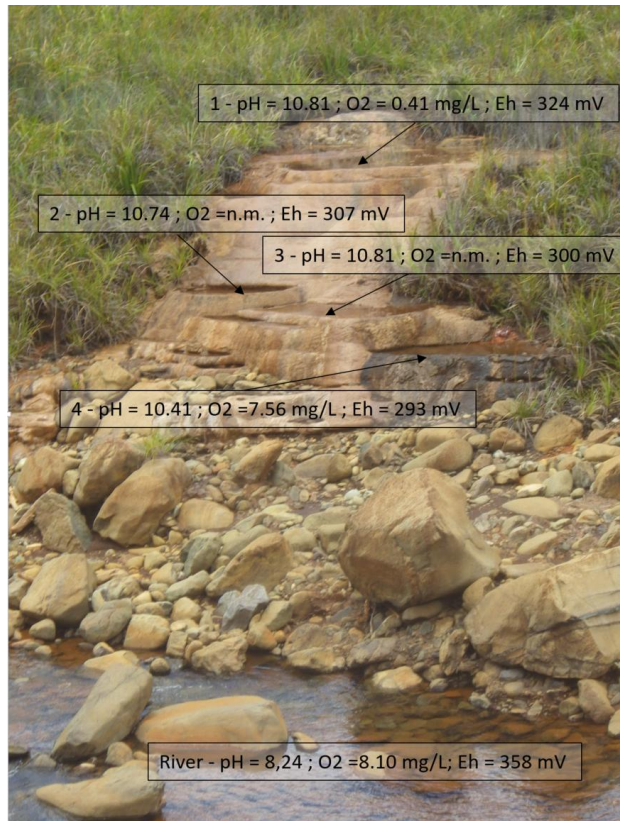
276

277 4.1.2 The dissolved oxygen content

278

279 At La Coulée, the water discharges in the upper pool from where it flows down to the other
 280 pools. The oxygen content of the water in the upper pool is 0.4 mg/L, 7.56 mg/L in the lower pool and
 281 8.24 mg/L in the river (Fig. 2). The Eh values are the same in all the pools. The water discharging at
 282 the upper pool becomes oxygenated by air uptake when it flows downhill. This air and thus the CO₂
 283 uptake lead to a small decrease in pH of 0.4 unit. Thus, for a given spring, variable values of *in situ*
 284 parameters can be obtained when measured away for the outlet.

285



286

287 *Figure 2 – The high-pH spring of La Coulée. The water discharges in the upper pool (1) and flows*
 288 *down toward the river through the upper (2) and lower (3) intermediate pools. It gets oxygenated on*

289 *the way, as indicated by the elevated O₂ content in the lower pool (4), at a value close to that of the*
290 *river. n.m.: not measured.*

291 The Pirogues and Coulée springs have similar oxygen content between 0.2 and 0.4 mg/L, which
292 classifies them as anoxic [Berner, 1981]. At the Montagne des Sources, the oxygen content of the very
293 large and deep pool is 3.0 mg/L while the water flowing at a fast rate from the outlet in the middle of
294 the formation (Fig. S1) is quite oxygenated (with a O₂(aq) content of 6.9 mg/L; Table S1).

295

296 4.1.3 The oxidation-reduction potential

297

298 The ORP values are measured in situ in reference to the Ag/AgCl standard. They have been
299 corrected for the potential difference between the Ag/AgCl and the hydrogen electrodes and thus
300 termed Eh (Fig. S2). There are marked differences in the Eh values between the springs, between the
301 days of measurement for the same spring and sometimes even within the time of recording (30 mn).

302 Eh at the spring Rivière des Pirogues has markedly varied between Dec. 2 and 12, 2014 (Fig
303 S1). There is also a small Eh maximum at Pirogues for the data of Dec. 2. Very sporadic bubbling (a
304 few events per hour) have been observed at La Coulée and also at the Pirogues site. For this latter
305 spring bubbles were observed not in the seepage of the spring where the water flows on the rocks
306 without being retained in a pool, but on the side of the very large pool (about 20 m wide) built by the
307 river about 10 meters downstream from the spring (Fig. S1). It has been shown in many instances that
308 gas bubbles forming in these high pH springs contain elevated concentrations of hydrogen (along with
309 methane and nitrogen). This has been documented for the Prony bay [Deville and Prinzhofer, 2016;
310 Monnin *et al.*, 2014]. We have observed at the Bain des Japonais in the Prony bay that gas bubbling
311 disrupts the ORP measurement when a gas bubble hits the probe. This may explain the Eh maximum
312 and the increase from -300 to -200 mv in Dec.2 at Pirogues (Fig. S1). This H₂-enriched gas venting
313 may also be the cause of the dispersion of the Eh values.

314

315 4.1.4 Comparison with other high-pH springs worldwide

316

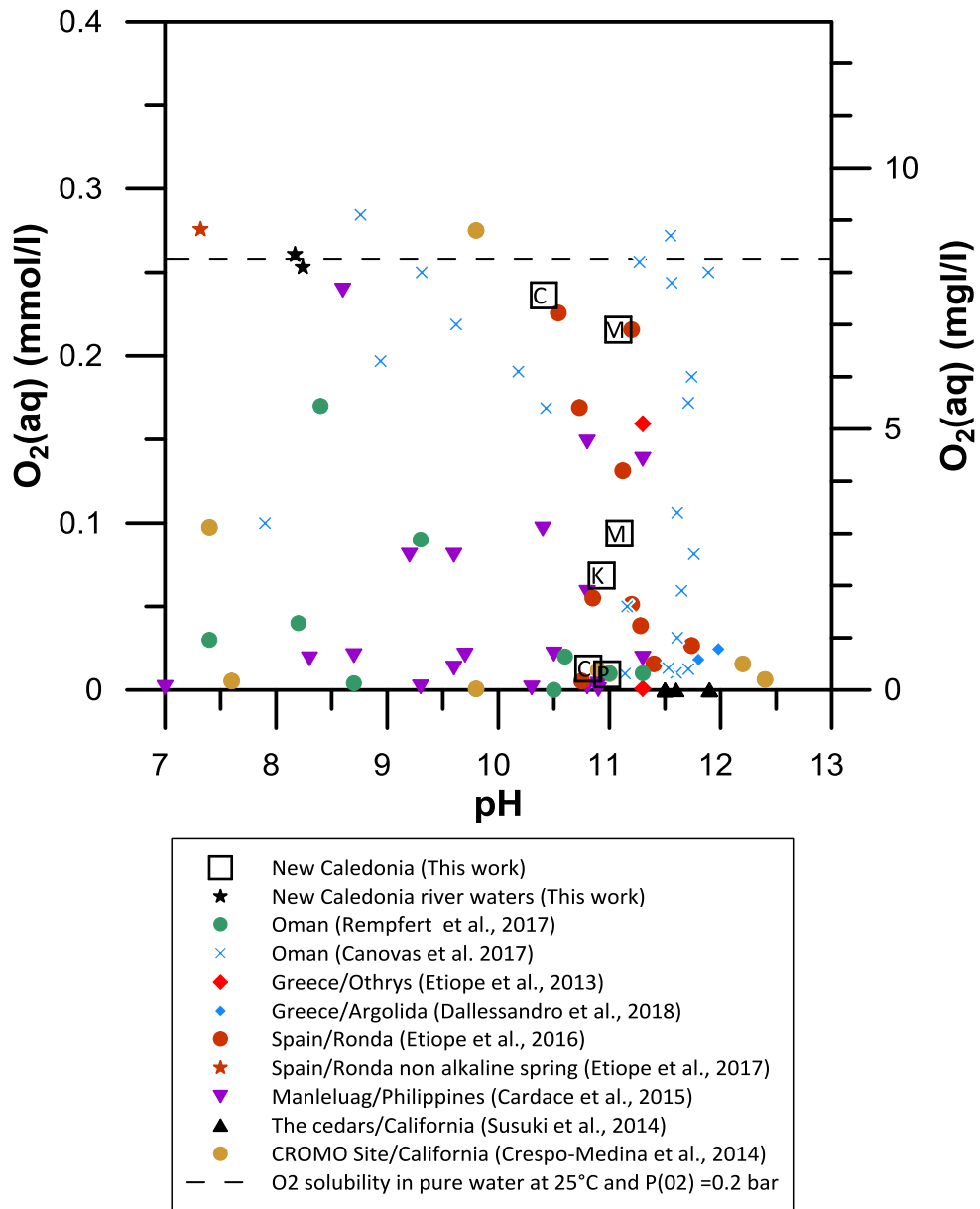
317 4.1.4.1 *The dissolved oxygen content*
318

319 Unfortunately, the dissolved oxygen concentration is not reported for every spring or seepage
320 area documented in the literature. The dissolved oxygen concentration of the New Caledonia springs
321 and of other high-pH springs worldwide are displayed versus pH in Fig. 3. These measurements were
322 made using different methods: with an oxygen probe (this work; [Cardace *et al.*, 2015; Etioppe *et al.*,
323 2016; Rempfert *et al.*, 2017; Suzuki *et al.*, 2013], on site spectrophotometric measurements based on
324 the indigo carmine reagent [Canovas *et al.*, 2017] and gas chromatography analysis of the dissolved
325 gases using the headspace method [Etioppe *et al.*, 2016]. In order to give the order of magnitude of
326 oxygen saturation, we used the dissolved oxygen content of pure water at equilibrium with the
327 atmosphere (i.e. for an oxygen partial pressure of 0.2 bar) at 25°C (8.3 mg/L) (Fig. 3). An accurate
328 calculation would require taking into account the temperature and the composition of the aqueous
329 phase (the Setchenov correction to Henry's constant). For example, oxygen solubility in pure water at
330 40°C is 6.41 mg/L. The three values reported for river waters close to the alkaline springs in New
331 Caledonia and a non-alkaline spring in Ronda (Spain; [Etioppe *et al.*, 2016]) are close to values of
332 oxygen saturation in pure water (Fig. 3). The present data for New Caledonia, but also the data for
333 Oman [Canovas *et al.*, 2017], for the Manleluag springs in the Philippines [Cardace *et al.*, 2015] and
334 for the Ronda springs in Spain [Etioppe *et al.*, 2016] show that at almost constant pH, the oxygen
335 content of the water samples collected in the high-pH springs can vary from zero to values close to
336 saturation. The waters at The Cedars springs in California [Suzuki *et al.*, 2013] and of the Argolida and
337 Othrys spring in Greece [D'Alessandro *et al.*, 2018a; Etioppe *et al.*, 2013] are either totally anoxic or
338 have a very low oxygen content. Water samples collected in boreholes in Oman [Rempfert *et al.*,
339 2017] or at the CROMO site (Coast Range Ophiolite Microbial Observatory) in Northern California
340 [Crespo-Medina *et al.*, 2014] are also oxygen free. The example of La Coulée spring show that
341 elevated dissolved oxygen concentrations measured away from the outlet result from atmospheric
342 oxygen dissolution due to air uptake. On the other hand, this air contamination provides carbon
343 dioxide to the water that contributes to the formation of the carbonate concretions building the pools
344 [Chavagnac *et al.*, 2013a; Leleu *et al.*, 2016]. Similarly, [Meyer-Dombard *et al.*, 2015] have shown

345 how the carbon content of the waters in the stream created by the discharge of a high pH fluid at
346 Chimarea springs (Turkey) increases with the distance from the source because of air uptake.

347 These data show that the high-pH waters discharging at the springs are oxygen-free, when they
348 are collected directly at the outlet. This is in agreement with the fact that oxygen is the first oxidant
349 consumed in the subsurface either through biological consumption or via the oxidation of ferric iron
350 [*Leong and Shock, 2020; Neal and Stanger, 1983*]. It is then concluded that the hydrologic system
351 discharging these high-pH waters is oxygen-free and that the venting gases should not contain any
352 oxygen. Therefore, the compositions of the gases venting at the seeps must then be corrected for this
353 air contamination.

354



355

356 *Figure 3 – The dissolved oxygen concentration of the New Caledonia hyperalkaline springs and*
 357 *of other springs worldwide. The dashed line is the value of oxygen saturation in pure water at 25°C.*

358 *The symbols for New Caledonia are: C = La Coulée, P = Pirogues, M = Montagne des Sources, K =*
 359 *Kaoris.*

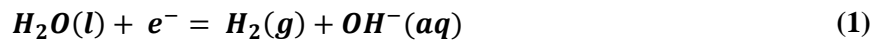
360

361 *4.1.4.2 The oxidation-reduction potential*

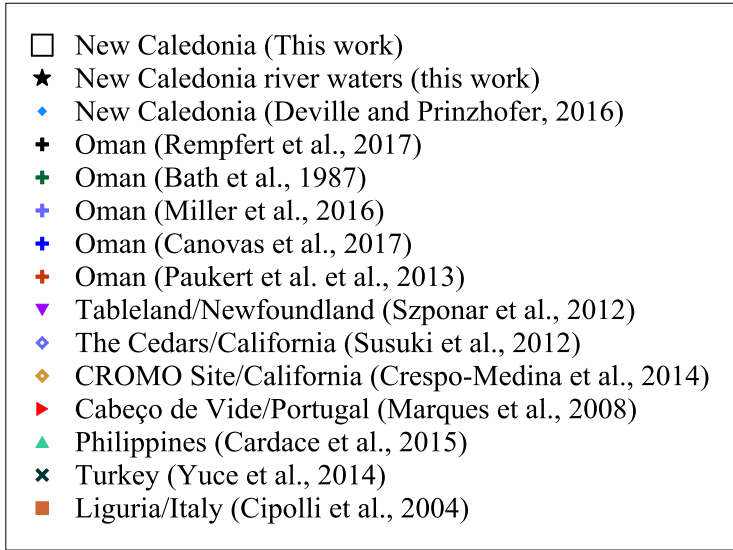
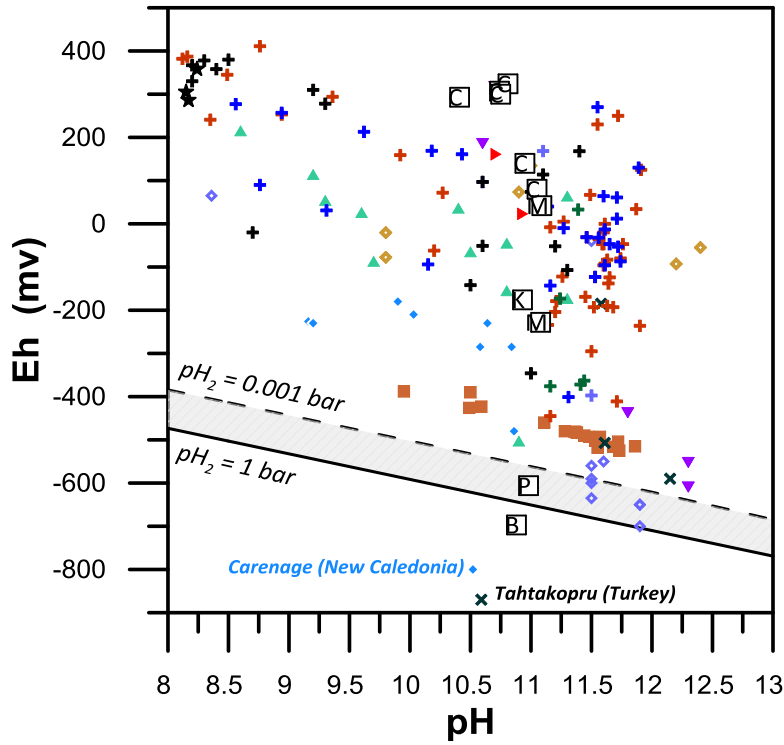
362

363 The data set is very scattered with no clear relationship between Eh and pH (Fig. 4). The redox
 364 conditions for the reduction of water are met for the Bain des Japonais and the Pirogues spring in New
 365 Caledonia (this work) and the Cedars springs in California. The ORP value for the Tahtakopru spring

366 of the Kilzidag ophiolite in Turkey [Yuce *et al.*, 2014] and for a spring called Carénage in New
367 Caledonia, which corresponds to the Bain des Japonais [Deville and Prinzhofer, 2016] are below the
368 water reduction limit, -800 mV for a pH of 10.52 and -870 mV for a pH of 10.59, respectively. There
369 is an ambiguity in the Eh values reported in the literature as the reference potential (Ag/AgCl or H₂) is
370 not always mentioned (e.g. [Paukert *et al.*, 2012]). Some of the values reported in Fig. 4 may be the
371 values given by the ORP probe (i.e. in reference to the Ag/AgCl standard) and thus may be too high
372 by about 200 mV (Fig. S2). Such a correction would bring the redox potential of the Carenage and
373 Tahtakopru springs close to the water reduction limit, i.e. corresponding to reaction (1):



374 These data show that these high-pH waters display the most reducing conditions at the surface
375 of the Earth. No correlation with the oxygen content of the waters was observed.



376

377 *Figure 4 – The oxidation-reduction potential Eh versus pH. The dashed lines correspond to the water*
 378 *reduction reaction (eq. 2) at 25°C for the two mentioned hydrogen partial pressures. The symbols for*
 379 *New Caledonia are: B= Bain des Japonais, C = La Coulée, P = Pirogues, M = Montagne des*
 380 *Sources, K = Kaoris. The Carenage spring is the name given to the Bain des Japonais by [Deville and*
 381 *Prinzhofer, 2016]. The Tahtakopru spring is one of the springs of the Kilzilgag ophiolite (Turkey;*
 382 *[Yuce et al., 2014]).*

383

384 4.2 The composition of the gases venting at the Bain des Japonais and Kaoris springs

385

386

387

388

389

390

391

392

393

The gas samples were collected between October, 2011 and November, 2014 at eight different dates in two springs of the Prony Bay (Table S2). At a given date, the concentration values are scattered, between 5 and 40% for H₂ and between 5 and 25% for CH₄ (Fig. 5). H₂ values are similar for the two springs, but CH₄ is lower at the Kaoris than at the Bain des Japonais. Some of the samples contain elevated concentrations of oxygen that we have attributed to air contamination (Table S2). Assuming that the nitrogen content of air is four times larger than its oxygen content and that air and the sampled gases are perfect gases, a corrected nitrogen content (in percentage) in each gas sample can be calculated using:

$$P_{N_2}(corr.) = P_{N_2}(raw) - 4 P_{O_2}(raw) \quad (2)$$

394

395

396

In eq. 2, “raw” designates the results of the chemical analysis (ionic chromatography). The hydrogen and methane concentrations are then recalculated using this corrected nitrogen concentration.

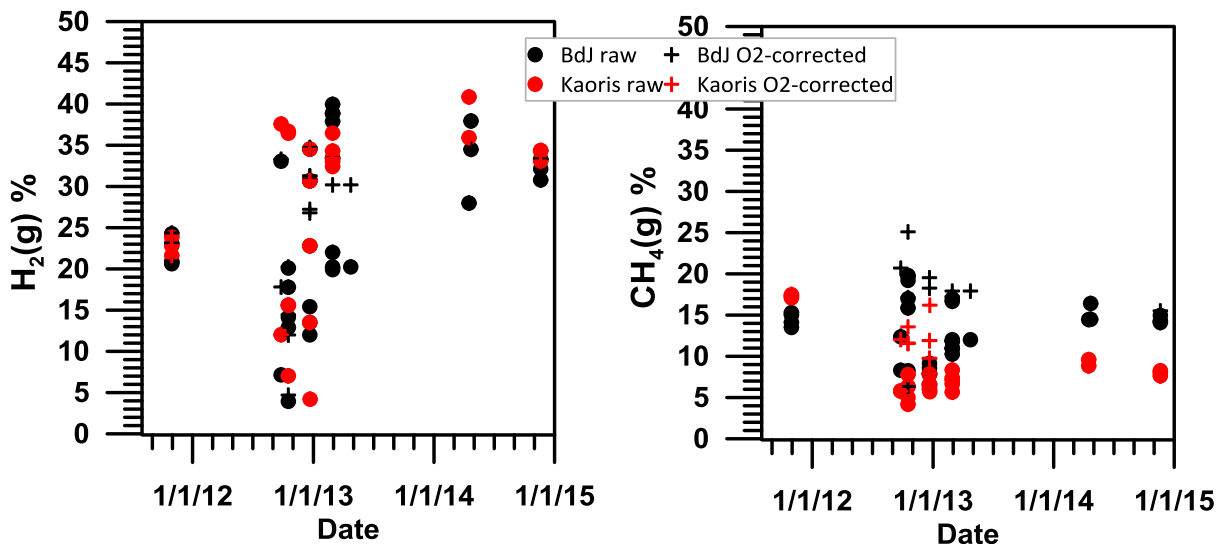
397

398

399

Data reveal a slightly increasing trend for H₂ and slightly decreasing for CH₄ during the four-year survey (Fig. 5). The scatter of the data is also due to the number of samples collected at a single date (Fig. 6).

400



401

402

Figure 5 – Uncorrected (filled dots) and O₂-corrected (crosses) hydrogen and methane contents

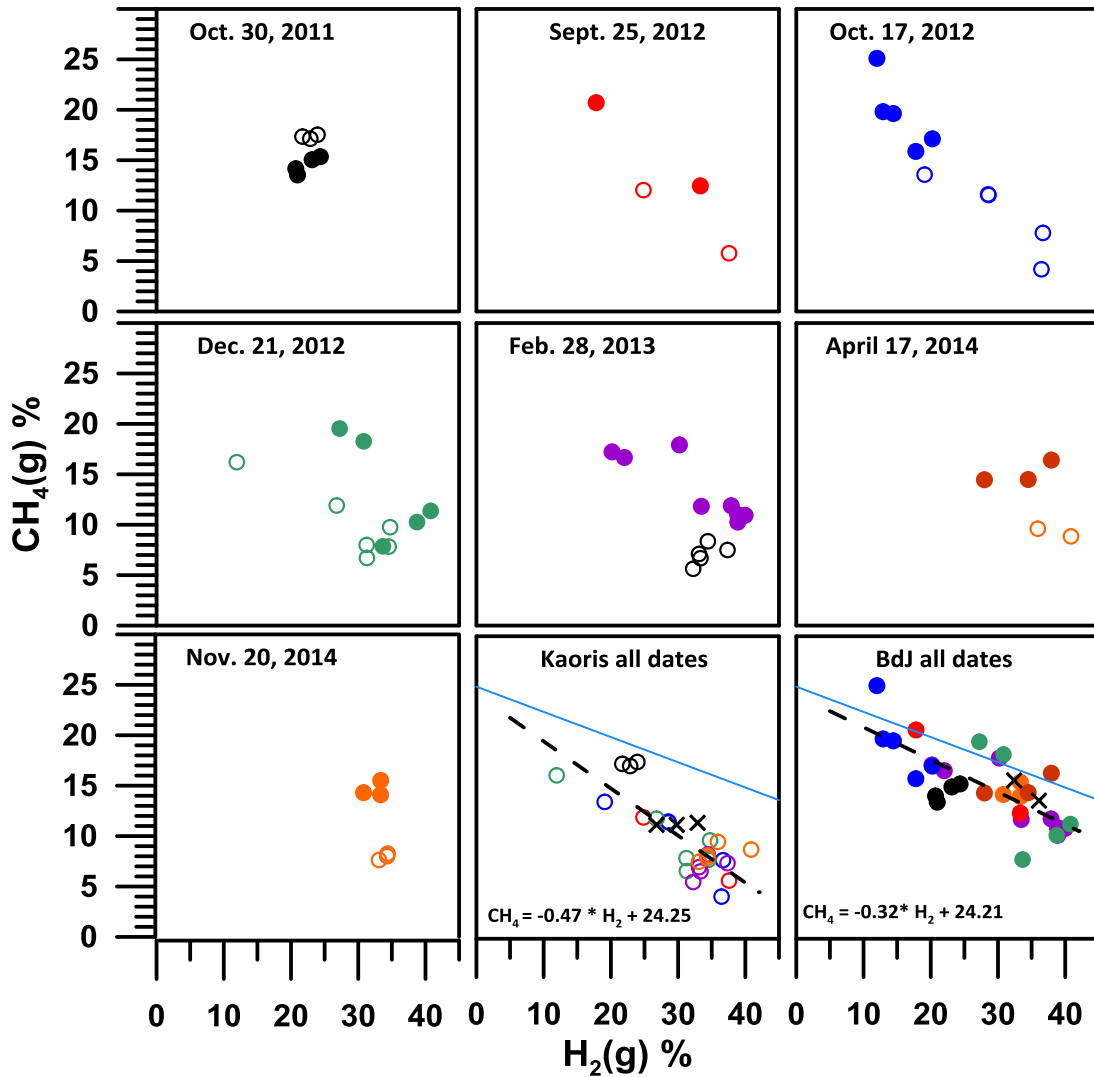
403

of the gases venting at the Bain des Japonais (black symbols) and at the Kaoris spring (red symbols).

404

405 When the number of samples collected at a given date allows it (e.g. Oct. 17, 2012; Table S2),
 406 the data show a correlation between the methane and hydrogen contents (Fig. 6). This correlation also
 407 appears on the entire data set, with different trends for the Kaoris and for the Bain des Japonais. Data
 408 depicted in Figs. 5 and 6 also show that the hydrogen content of the gases can fluctuate during the time
 409 of sampling on a given day, for example between 20 and 35% on Oct. 17, 2012. Because gas flow is
 410 steady at these two springs, it takes less than half an hour to collect 5 samples. It also shows that the
 411 conversion of hydrogen to methane (see below) is also very rapid, otherwise the methane
 412 concentration would not be correlated to that of hydrogen. In future studies, it will be necessary to
 413 note, not only the date of sampling, but also the hour.

414



415

416 *Figure 6 – The CH₄(g) concentration of the Bain des Japonais and the Kaoris springs versus*
 417 *that of H₂(g) for each date and for the whole data set. Open dots: Kaoris; filled dots: Bain des*
 418 *Japonais (BdJ); crosses: Vacquand et al. 2018. The dashed lines are fits to the data and the formulas*
 419 *are the expressions of the linear regressions. The plain lines represent the variation of the methane*
 420 *and hydrogen concentrations due to the reaction of fully oxidized carbon (such as CO₂) with hydrogen*
 421 *to produce methane, thus with a slope of -0.25 (see text and Fig. 7).*

422

423 4.3 A comparison of the gas composition of New Caledonia alkaline springs with 424 similar sites worldwide

425

426 Gas venting is commonly observed in hyperalkaline springs, but not in all of them. Whereas it is
 427 revealed by bubbles in spring waters, it can be detected as “dry” seeps in serpentinized peridotites
 428 [Zgonnik et al., 2019]. The compositions of free gases venting in Oman, Italy (Liguria and Elba
 429 Island), Turkey and the Philippines have been corrected for O₂ contamination and recalculated for the
 430 N₂-H₂-CH₄ system, as done for New Caledonia (Fig. 7; see plots for each location in Fig. S3). It has
 431 already been shown that gases can be classified into a few types, such as H₂-rich, CH₄-rich or N₂-rich
 432 [Boulart et al., 2013; D'Alessandro et al., 2018b; Deville and Prinzhofer, 2016; Vacquand et al.,
 433 2018].

434 The present data point to three categories (Fig. 7):

435 1) Gases with little or no hydrogen (CH₄-N₂ gases). The methane content of these CH₄-N₂ gases
 436 varies within a large range, between 0 and 100%. They are found in the Voltri ophiolite in Liguria
 437 (Northern Italy; [Boschetti et al., 2013; Boulart et al., 2013; Etiope and Whiticar, 2019], in the
 438 Gulderen and Gokdere springs of the Kilzidag ophiolite in Turkey [D'Alessandro et al., 2018b], in the
 439 submarine seeps offshore the Elba Island (Italy; [Sciarra et al., 2019], in the sample collected at the
 440 submarine Aiguille de Prony in the Prony Bay in New Caledonia [Vacquand et al., 2018] and in the
 441 Chimarea seeps (Turkey) where venting gases are almost pure methane with less than 10% of either
 442 N₂ or H₂ [Etiope et al., 2011; Vacquand et al., 2018]. [Vacquand et al., 2018] report the very peculiar
 443 composition of a gas sample of the Aiguille de Prony (New Caledonia) collected in the vial containing

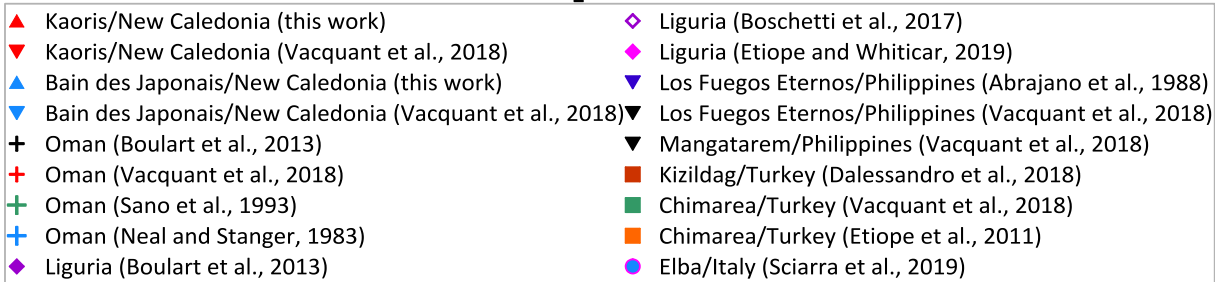
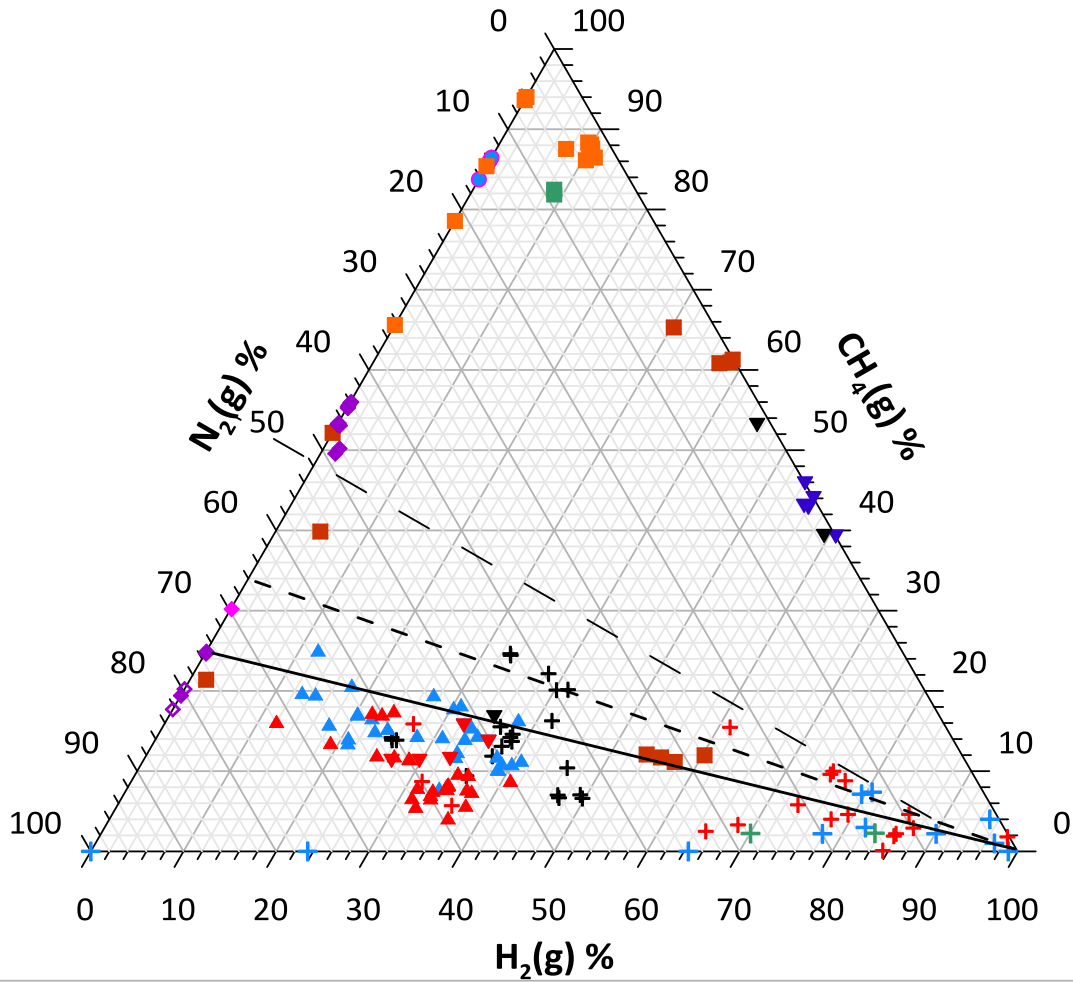
444 a degassing water, and as such not a free gas sample *per se*. It contains no hydrogen and only a very
445 small quantity (5%) of methane and as such is almost pure nitrogen. Several samples collected in
446 Oman by [Neal and Stanger, 1983] are merely air, but the gas sample pure nitrogen at the Huwayl
447 Qufays spring is pure nitrogen.

448 2) Gases with little or no nitrogen ($\text{CH}_4\text{-H}_2$ gases). They vent in the dry seeps of Los Fuegos
449 Eternos and Nagsasa Bay in the Philippines [Abrajano *et al.*, 1988; Vacquand *et al.*, 2018], of the
450 Kurtbagi area in the Kilzidag ophiolite (Turkey; [D'Alessandro *et al.*, 2018b; Yuce *et al.*, 2014] and
451 also of the Chimarea seeps (Turkey; [Etiopie *et al.*, 2011; Vacquand *et al.*, 2018]).

452 3) The compositions of gases collected in New Caledonia (this work; [Vacquand *et al.*, 2018]),
453 in Oman [Boulart *et al.*, 2013; Neal and Stanger, 1983; Sano *et al.*, 1993; Vacquand *et al.*, 2018], at
454 the Mangatarem site in the Zambales ophiolite (Philippines; [Vacquand *et al.*, 2018]), and at the
455 Tahtakopru springs of the the Kilzidag ophiolite (Turkey; [D'Alessandro *et al.*, 2018b]) can be grouped
456 into the $\text{N}_2\text{-H}_2\text{-CH}_4$ type. They build a trend from almost pure hydrogen, as found in Oman, to $\text{N}_2\text{-CH}_4$
457 gases containing no hydrogen and no more than 20% of methane, as found in Liguria at Acquasanta
458 [Etiopie and Whiticar, 2019], Branaga [Boschetti *et al.*, 2013] and GOR35 (one of the springs of Lago
459 Lavagnina; [Boulart *et al.*, 2013]) and at Gulderen spring of the Kilzidag ophiolite [D'Alessandro *et*
460 *al.*, 2018b]. Free gases for which hydrogen is dominant (>60%) have been collected in Oman by
461 [Sano *et al.*, 1993] in 1982-1983 and by [Neal and Stanger, 1983] at dates that are not mentioned, but
462 likely at the same period as Sano *et al.*, and by [Vacquand *et al.*, 2018] between 2008 and 2012. While
463 these data are in fair agreement at high hydrogen content, in spite of the scatter, they differ at
464 hydrogen concentrations below 60%. [Boulart *et al.*, 2013] report Omani gas compositions with
465 hydrogen concentrations lower than those reported by [Vacquand *et al.*, 2018], although the samples
466 have been collected mostly at the same locations. The three points with the lowest H_2 contents
467 ($20 < \text{H}_2 < 40\%$) are nevertheless in agreement. Also, the data for New Caledonia reported by these two
468 research groups [Boulart *et al.*, 2013; Vacquand *et al.*, 2018] are in full agreement, so that it is
469 unlikely that these differences for Oman are due to different sampling or analytical methods.

470

471



472

473 *Figure 7 – A triangular plot of the O₂-corrected free gas compositions in serpentizing*
 474 *environments. The black plain line is the line with a slope of -0.25 corresponding to the Sabatier*
 475 *reaction involving CO₂. The short dash line has a slope of -0.33 corresponding to a Fisher-Tropsch-*
 476 *type reaction involving carbon monoxide (see text). The long dash line represents the reaction of*
 477 *elemental carbon with hydrogen (slope -0.5).*

478

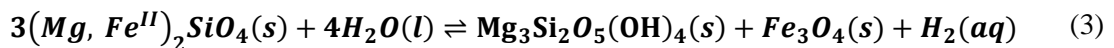
479 5 Discussion

480

481 The present analysis of the free gas composition is based on the observation that the endmember
 482 high-pH waters discharging at the springs are totally devoid of oxygen, meaning that oxygen is
 483 consumed in the subsurface and that gases venting at the surface should also be oxygen-free. Small
 484 amounts of oxygen would not drastically change the correction (eq. 2). Oxygen is very rapidly
 485 consumed when oxic waters flow into geological formations (see the examples of oxygen dynamics in
 486 karstic environments; [Monnin *et al.*, 2019; Young *et al.*, 2018]). This lends support to the conclusion
 487 that the hydrothermal systems responsible for the discharge of high-pH waters at the surface are
 488 anoxic.

489 The composition of gas samples collected the same day at a given spring in New Caledonia is
 490 variable (Fig. 6). Such a very rapid (hourly) variation of the hydrogen concentration of gases emitted
 491 at the surface has been documented in the so-called “fairy circles” in Brazil [Myagkiy *et al.*, 2020].
 492 The hydrogen concentration is roughly increasing (and the methane roughly decreasing) with time, for
 493 the period of the survey (3 years). The four data sets for the Oman gas samples have been sampled at
 494 dates that span from the early eighties ([Neal and Stanger, 1983; Sano *et al.*, 1993] to the beginning
 495 of the years 2010 [Boulart *et al.*, 2013; Vacquand *et al.*, 2018]. All these data point to a time variation
 496 of the free gas compositions, that for now cannot be related to seasonal or climatic change but
 497 certainly reveal the dynamics of the hydrothermal system. Only long-term monitoring, with
 498 measurements at high frequency can provide further insight into this variation.

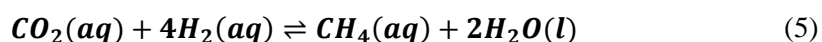
499 Serpentinization is the aqueous alteration of metallic minerals such as olivine to produce
 500 serpentine. It can be represented by:



501 This reaction produces hydrogen, which at first is dissolved (which is indicated by $\text{H}_2(\text{aq})$ in Eq. 3).
 502 When the hydrogen concentration reaches the saturation value, a gas phase is produced (degassing,
 503 bubbling):



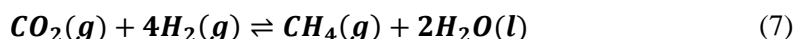
504 Hydrogen can react with carbon-containing substances to produce methane. There are several ways to
 505 write this hydrogen consumption. All of them represent a well-defined mechanism. They also place
 506 strong constraints on the nature (for example carbon oxidation state) and the physical state (aqueous or
 507 gaseous) of the reactants. For example, hydrogen consumption to give methane through
 508 hydrogenotrophic methanogenesis (thus driven by methanogens), and therefore necessarily in the
 509 aqueous phase, can be represented by:



510 In eq. 5, carbon is totally oxidized, for example as in carbonic acid. Again the methane concentration
 511 in the aqueous phase can reach the saturation value and methane will degas:

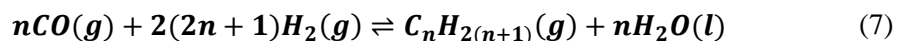


512 A methane production in the gas phase could be written in a similar way, which corresponds to the
 513 Sabatier reaction:

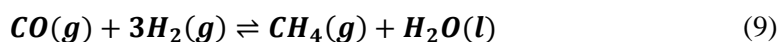


514 Strictly speaking, the Sabatier reaction is a catalyzed process at elevated temperatures (400-500°C)
 515 converting carbon dioxide into methane (methanation). Both Eqs. 6 and 7 have the same
 516 stoichiometry: four moles of hydrogen are consumed to produce one mole of methane. In a plot of the
 517 methane versus the hydrogen content this would be represented by a line with a slope of -0.25.

518 The Fisher-Tropsch reaction is the conversion of carbon monoxide into alkanes:

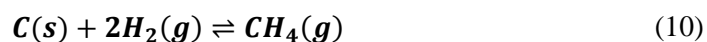


519 One of the criteria distinguishing the Sabatier reaction from the Fisher-Tropsch process is that the first
 520 one leads to an almost pure methane (methanation) while the second one leads to a more complex
 521 mixture of higher alkanes. Methane production following a Fisher-Tropsch scheme can be written as:



522 In a plot of the methane versus the hydrogen content of the gas, eq. 9 would be represented by a line
 523 with a slope of -0.33.

524 Elemental carbon has been considered as a possible source of carbon in methane production in
 525 serpentinizing environments (e.g. [Vacquand *et al.*, 2018]):



526 Reaction 10 consumes two moles of hydrogen to produce one mole of methane, thus leading to a line
 527 with a slope -0.5 in a methane versus hydrogen plot.

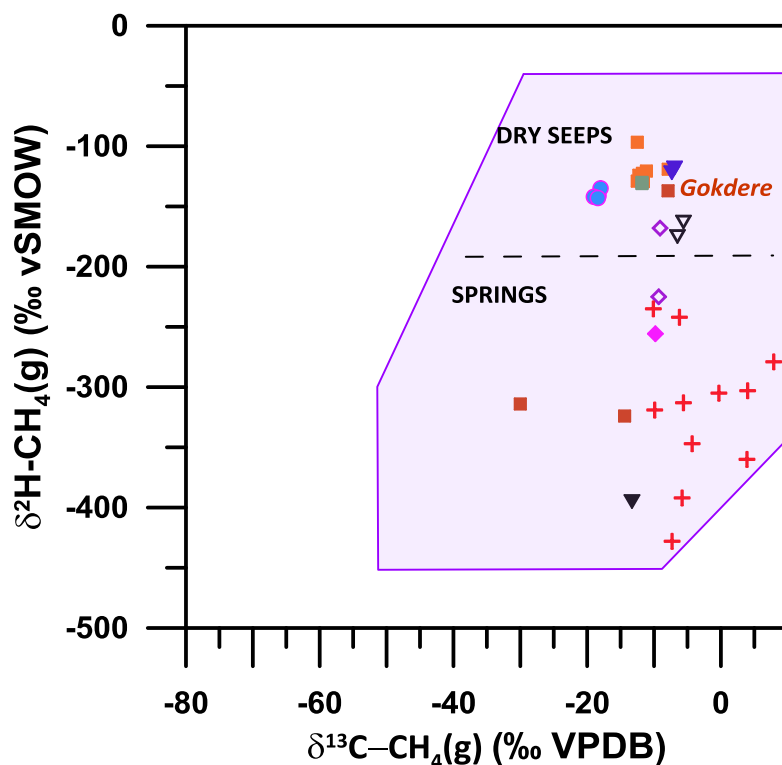
528 Serpentinization can be described as a process starting with the production of hydrogen (eq. 3)
 529 followed by hydrogen consumption, either in the gas phase (eq. 7) or in an aqueous solution (eq. 5) to
 530 produce methane. The data reported in Fig 7 are more consistent with the stoichiometry of the
 531 reactions involving fully oxidized carbon (eq. 5 and 7) than with those involving less oxidized carbon
 532 (eq. 8) or reduced carbon (eq. 9). As such, in a strict sense, it should be termed Sabatier-type reaction
 533 instead of Fischer-Tropsch type (FFT). This distinction is more significant than what it seems as it
 534 directly relates to the ongoing debate on the nature of the carbon source in low temperature
 535 serpentinization. Increasingly complex reaction schemes and carbon substrates are now contemplated
 536 and discussed (e.g. [Menez, 2020; Reeves and Fiebig, 2020]).

537 Yet this correlation between the hydrogen and methane contents of the H₂-CH₄-N₂ gases does
 538 not distinguish a process taking place in the gas phase from a reaction in an aqueous solution followed
 539 by degassing. It also implies that nitrogen is produced simultaneously with hydrogen consumption and
 540 methane formation. If this was not the case, for example if nitrogen was coming from deeper sources
 541 such as sediments, crustal or mantle rocks below the ophiolites [Vacquand *et al.*, 2018], it would be
 542 found in all samples so that H₂-rich gases would be diluted by this deeply-sourced nitrogen and their
 543 composition would move away from the pure H₂ apex and from the CH₄-H₂ gas type (Fig. 7). **It can be
 544 proposed that the chemical changes brought by serpentinization provide the necessary conditions for
 545 the production of gaseous nitrogen from dissolved nitrate, i.e. denitrification. Such a process which is
 546 mediated by bacteria at surface conditions, has not been studied so far in hyperalkaline environments.**

547 The data for the Kaoris spring (and to a lesser extend for the Bain des Japonais) (this work)
 548 show a CH₄ content lower than the stoichiometry of the Sabatier reaction (Fig. 7; Fig S3). This can be

549 attributed to a consumption of methane, but it is difficult to consider such a consumption in the gas
550 phase (apart from burning). Methanotrophs and methanogens have already been identified in several
551 alkaline springs such as Prony Bay (in both Kaoris and Bain des Japonais springs) [Frouin *et al.*,
552 2018; Mei *et al.*, 2016; Postec *et al.*, 2015; Quemeneur *et al.*, 2014], the Voltri ophiolite (Liguria,
553 Italy) [Brazelton *et al.*, 2017; Quéméneur *et al.*, 2015], the Santa Elena ophiolite (Costa Rica)
554 [Crespo-Medina *et al.*, 2017], the Oman ophiolite ([Kraus *et al.*, 2020; Rempfert *et al.*, 2017]; Kraus *et*
555 *al.*, 2020) and the Cedars springs (California) [Suzuki *et al.*, 2013]. Methane consumption or
556 production by microorganisms take place in the aqueous phase. Again transfer of gases from the gas
557 phase to the aqueous phase (and conversely) plays a role in the methane and hydrogen budget of the
558 system. It would be erroneous to conclude that a Sabatier-type reaction in the gas phase necessarily
559 implies an overall abiotic formation of methane.

560 The origin of methane (abiotic, biogenic, thermogenic, magmatic) can be inferred from a variety
561 of criteria, each of them with its advantages and pitfalls (e.g. [Etiopie and Whiticar, 2019; Reeves and
562 Fiebig, 2020]). Gases venting in fractures (dry) seeps and in springs were suggested to belong to the
563 abiotic methane domain in a $\delta^2\text{H}$ versus $\delta^{13}\text{C}$ diagram [Vacquand *et al.*, 2018]. Data for Oman,
564 Philippines, Liguria, Turkey and Elba Island indeed plot within the of abiotic field empirically defined
565 from isotopic data for methane venting in serpentinizing environments [Milkov and Etiopie, 2018] (Fig.
566 8). This field has likely been delimited in part using the same data as reported in Fig. 8. Unfortunately
567 the study of Milkov and Etiopie does not provide a simple way of tracking down the data used to
568 delimit the abiotic methane domain. This field can be subdivided into the dry seeps and the springs
569 [Vacquand *et al.*, 2018]. Note that the Gokdere spring of the Kildizag ophiolite (Turkey) lies in the
570 “dry seeps” domain.



+	Oman (Vacquant et al., 2018)	▼	Mangatarem/Philippines (Vacquant et al., 2018)
◇	Liguria (Boschetti et al., 2017)	■	Kizildag/Turkey (Dalessandro et al., 2018)
◆	Liguria (Etiope and Whiticar, 2019)	■	Chimarea/Turkey (Vacquant et al., 2018)
▼	Los Fuegos Eternos/Philippines (Abrajano et al., 1988)	■	Chimarea/Turkey (Etiope et al., 2011)
▽	Los Fuegos Eternos/Philippines (Vacquant et al., 2018)	●	Elba/Italy (Sciara et al., 2019)

571

572 *Figure 8 – The δ^2* The hydrogen-methane relationship can also be seen as a picture of different
 573 stages of the evolution of the hyperalkaline hydrothermal systems in different regions, as a result of
 574 the local hydrological conditions, differences in lithology thus leading to different residence times of
 575 the waters and the gases in the subsurface. It can be speculated that the H_2 -rich gases in Oman would
 576 then be the first step, after which methane starts forming in increasingly large amounts up to the point
 577 where all the hydrogen is consumed to reach the end point of the CH_4-N_2 gases.

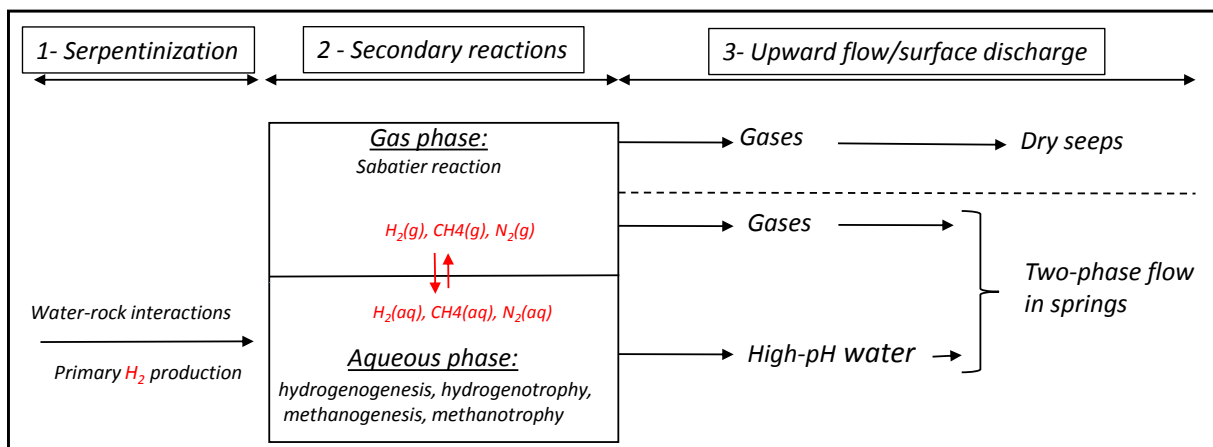
578 It is also very likely that the flow path and the rate of flow of gases and waters are different.
 579 Etiope and Whiticar (2019) have shown that the carbon in the methane is older than 50 000 years as it
 580 is ^{14}C free whereas the age of the waters in hyperalkaline springs determined from ^{14}C in aqueous
 581 carbonate is only a few thousand years. As such this infers in an apparent decoupling of the sources of
 582 the waters and gases sampled at the surface. Serpentinization is an aqueous alteration process, so that
 583 hydrogen is first produced in an aqueous (liquid) environment. A gas phase will form only when the

584 hydrogen concentration exceeds saturation. The formation of methane may take place in this gas
 585 phase, as proposed by Etiope and Whiticar (2019). Methane can then dissolve into the water and be
 586 used as a substrate by methanotrophs.

587 Figure 9 presents a diagram that summarizes the observations and conclusions of this work. It
 588 highlights the relationship between the gas and aqueous phases, but cannot explain the reason why
 589 gases in dry seeps do not contain nitrogen. **The $\delta^2\text{H}$ and $\delta^{13}\text{C}$ isotope data (Fig. 8) point to isotopic**
 590 **$\delta^2\text{H}\text{-CH}_4(\text{g})$ signatures different for dry seeps than those for springs. This may indicate different**
 591 **mechanisms at play in the generation of methane.** Serpentinization is the first step of the water-rock
 592 interactions during which hydrogen is generated by the reduction of water and the oxidation of metals.
 593 Because it is an aqueous process, hydrogen is forming within the aqueous phase, and a gas phase will
 594 form only when its concentration exceeds saturation. Methane can then be generated within this gas
 595 phase by a Sabatier reaction. Methane will dissolve into the aqueous solution where it can support the
 596 development of methanotrophs. The methane budget in the gas will be due to its production by the
 597 Sabatier process and its consumption by its dissolution in the water. In the aqueous phase, the methane
 598 budget will result from its uptake from the gas phase, its consumption by methanotrophs, but also its
 599 formation by potential methanogens.

600 Clumped isotope data for CH_4 and an analysis of the dissolved gas data will be reported in
 601 separate publications.

602



603

604 *Figure 9 – A diagram summarizing the hydrogen, methane, and nitrogen budgets in the serpentinizing*
 605 *environment. The first step is hydrogen production by the serpentinization reaction. The hydrogen*
 606 *concentration increases in the water up to the point where saturation is exceeded, and a gas phase*
 607 *forms. In Step 2, methane is produced by a secondary process with the stoichiometry of the Sabatier*
 608 *reaction. Nitrogen is also produced during this step (see text). The gases are reactive in both the gas*
 609 *and the aqueous phases and their concentrations are linked by a solubility relationship. In the last*
 610 *step (3) gases and water flow toward the surface to discharge at dry seeps and springs.*

611

612 6 Conclusions

613

614 • The dissolved oxygen concentrations measured *in situ* in the New Caledonia on-land springs
 615 along with literature data on alkaline springs worldwide show that high-pH waters discharging
 616 at the springs are anoxic. Therefore gases venting at the spring should also not contain any
 617 oxygen. It is then necessary to correct gas compositions for atmospheric oxygen
 618 contamination.

619 • The compositions of gases collected at the Kaoris and Bain des Japonais springs in New
 620 Caledonia over a four-year period (2011–2014) show daily variations and some trends during
 621 the duration of the survey. Free gases collected in Oman by four different research groups
 622 over a period of about 20 years also display varying compositions. It can be cautiously
 623 concluded that there is a time variation of composition of free gases venting in these
 624 serpentinizing environments, at the hour scale as well as at the seasonal or yearly scale.

625 • The hydrogen and methane contents of free gases collected in New Caledonia along with
 626 those of Oman, the Mangatarem (Philippines) spring and the Tahtakopru (Turkey) springs
 627 define a trend of H₂-CH₄-N₂ gases going from almost pure hydrogen to N₂-CH₄ gases (with
 628 CH₄ around 25%). The slope of this trend is consistent with the stoichiometry of methane
 629 production from an oxidized carbon source such as carbon dioxide or carbonic acid. It also
 630 implies that nitrogen is produced simultaneously with methane.

631 • The stoichiometry of the hydrogen-methane reaction is consistent with a Sabatier reaction in
 632 the gas phase or a methane production by hydrogenotrophic methanogens in the aqueous

633 phase. The two mechanisms can take place at the same time and can be coupled through the
634 transfer of gases from the water to the gas phase and conversely. This last point can be
635 constrained by the study of the concentration of dissolved gases to investigate the conditions
636 at which the water degasses.

637

638

639 ACKNOWLEDGEMENTS

640 The authors declare no conflict of interest. The survey of the springs has been funded by the Grand

641 Observatoire du Pacifique Sud (GOPS). This work has also been supported by the INTERVIE

642 program of Institut des Sciences de la Terre et de l'Univers (INSU/CNRS) and the French Institute of

643 Research for Development (IRD). We thank the environmental service of the Province Sud of New

644 Caledonia for the authorization to sample the springs. We thank Michael Kubo and Tori Hoehler of

645 NASA Ames laboratory for their help with the gas analyses. We deeply acknowledge the help and

646 support of the sea means service (pilots Miguel Clarque and Samuel Tereua) and the diving service

647 (divers Eric Folcher, Bertrand Bourgeois and Armelle Renaud) of the IRD center of Nouméa, New

648 Caledonia, for the logistics of the sampling campaigns. We also warmly thank Jean Chatelier who

649 organized the logistics and visit to the Montagne des Sources.

650 The supplementary information for this paper is availablel at the CNRS HAL archive

651 (<https://hal.archives-ouvertes.fr/>).

652

653

654 **References**

655

656 Abrajano, T. A., N. C. Sturchio, J. K. Bohlke, G. L. Lyon, R. J. Poreda, and C. M. Stevens (1988),

657 Methane-hydrogen gas seeps, Zambales Ophiolite, Philippines: Deep or shallow origin?, *Chemical*658 *Geology*, 71(1-3), 211-222.

659 Alexander, W. R., R. Dayal, K. Eagleson, J. Eikenberg, E. Hamilton, C. M. Linklater, I. G. McKinley, and

660 C. J. Tweed (1992), A NATURAL ANALOG OF HIGH PH CEMENT PORE WATERS FROM THE MAQARIN

661 AREA OF NORTHERN JORDAN .2. RESULTS OF PREDICTIVE GEOCHEMICAL CALCULATIONS, *Journal of*662 *Geochemical Exploration*, 46(1), 133-146, doi:10.1016/0375-6742(92)90104-g.663 Berner, R. A. (1981), A new geochemical classification of sedimentary environments, *Journal of*664 *Sedimentary Research*, 51(2), 359-365, doi:10.1306/212F7C7F-2B24-11D7-8648000102C1865D.

665 Blank, J. G., G. Etiope, V. Stamenković, A. R. Rowe, I. Kohl, S. Li, and E. D. Young (2017), Methane at

666 the Aqua de Ney Hyperalkaline Spring (N. California USA), a Site of Active Serpentinization, in

667 *Astrobiology Science Conference 2017*, edited, p. Abstract #3608, Lunar and Planetary Institute,

668 Houston.

669 Boschetti, T., G. Etiope, and L. Toscania (2013), Abiotic methane in the hyperalkaline springs of

670 Genova, Italy., *Procedia Earth and Planetary Science*, 7, 248-251.

671 Boschetti, T., and L. Toscani (2008), Springs and streams of the Taro-Ceno Valleys (Northern

672 Apennine, Italy): Reaction path modeling of waters interacting with serpentinized ultramafic rocks,

673 *Chemical Geology*, 257(1-2), 76-91.

674 Boschetti, T., L. Toscani, P. Iacumin, and E. Selmo (2017), Oxygen, Hydrogen, Boron and Lithium

675 Isotope Data of a Natural Spring Water with an Extreme Composition: A Fluid from the Dehydrating

676 Slab?, *Aquatic Geochemistry*, doi:10.1007/s10498-017-9323-9.

677 Boulart, C., V. Chavagnac, C. Monnin, A. Delacour, G. Ceuleneer, and G. Hoareau (2013), Differences

678 in gas venting from ultramafic-hosted warm springs: the example of Oman and Ligurian Ophiolites,

679 *Ophioliti*, 38(2), 142-156.

680 Brazelton, W. J., C. N. Thornton, A. Hyer, K. I. Twing, A. A. Longino, S. Q. Lang, M. D. Lilley, G. L. Fruh-

681 Green, and M. O. Schrenk (2017), Metagenomic identification of active methanogens and

682 methanotrophs in serpentinite springs of the Voltri Massif Italy, *PeerJ*, 5, 33, doi:10.7717/peerj.2945.

683 Canovas, P. A., T. Hoehler, and E. L. Shock (2017), Geochemical bioenergetics during low-temperature

684 serpentinization: An example from the Samail ophiolite, Sultanate of Oman, *J. Geophys. Res.-*685 *Biogeosci.*, 122(7), 1821-1847, doi:10.1002/2017jg003825.

686 Cardace, d., D. A. R. Meyer-Dombard, K. Woycheese, and C. A. Arcilla (2015), Feasible Metabolic

687 Schema Associated with High pH Springs in the Philippines, *Frontiers in Microbiology*, 6,

688 doi:10.3389/fmicb.2015.00010.

689 Chavagnac, V., G. Ceuleneer, C. Monnin, B. Lansac, G. Hoareau, and C. Boulart (2013a), Mineralogical

690 assemblages forming at hyper-alkaline warm springs hosted on ultramafic rocks: a case study of

691 Oman and Ligurian ophiolites, *Geochemistry, Geophysics, Geosystems* 14(7), 2474–2495,.

692 Chavagnac, V., C. Monnin, G. Ceuleneer, C. Boulart, and G. Hoareau (2013b), Characterization of

693 hyperalkaline fluids produced by low temperature serpentinization of mantle peridotites in the

694 Oman and Ligurian ophiolites., *Geochemistry Geophysics Geosystems*, 14(7), 2496–2522.

695 Christofi, C., A. Bruggeman, C. Kuells, and C. Constantinou (2020), Hydrochemical evolution of

696 groundwater in gabbro of the Troodos Fractured Aquifer. A comprehensive approach, *Applied*697 *Geochemistry*, 114, 104524, doi:<https://doi.org/10.1016/j.apgeochem.2020.104524>.

698 Cipolli, F., B. Gambardella, L. Marini, G. Ottonello, and M. Vetuschi Zuccolini (2004), Geochemistry of

699 high-pH waters from serpentinites of the Gruppo di Voltri (Genova, Italy) and reaction path modeling

700 of CO₂ sequestration in serpentinite aquifers, *Applied Geochemistry*, 19(5), 787-802.

701 Cox, M. E., J. Launay, and J. P. Paris (1982), Geochemistry of low temperature geothermal systems in

702 New Caledonia, paper presented at Pacific Geothermal Conference, University of Auckland,

703 Auckland, 1982.

- 704 Crespo-Medina, M., K. I. Twing, M. D. Y. Kubo, T. M. Hoehler, D. Cardace, T. McCollom, and M. O.
 705 Schrenk (2014), Insights into environmental controls on microbial communities in a continental
 706 serpentinite aquifer using a microcosm-based approach, *Frontiers in Microbiology*, 5(604),
 707 doi:10.3389/fmicb.2014.00604.
- 708 Crespo-Medina, M., K. I. Twing, R. Sanchez-Murillo, W. J. Brazelton, T. M. McCollom, and M. O.
 709 Schrenk (2017), Methane Dynamics in a Tropical Serpentinizing Environment: The Santa Elena
 710 Ophiolite, Costa Rica, *Frontiers in Microbiology*, 8, doi:10.3389/fmicb.2017.00916.
- 711 D'Alessandro, W., K. Daskalopoulou, S. Calabrese, and S. Bellomo (2018a), Water chemistry and
 712 abiogenic methane content of a hyperalkaline spring related to serpentinization in the Argolida
 713 ophiolite (Ermioni, Greece), *Marine and Petroleum Geology*, 89, 185-193,
 714 doi:10.1016/j.marpetgeo.2017.01.028.
- 715 D'Alessandro, W., G. Yüce, F. Italiano, S. Bellomo, A. H. Gülbay, D. U. Yasin, and A. L. Gagliano
 716 (2018b), Large compositional differences in the gases released from the Kizildag ophiolitic body
 717 (Turkey): Evidences of prevalingly abiogenic origin, *Marine and Petroleum Geology*, 89, 174-184,
 718 doi:<https://doi.org/10.1016/j.marpetgeo.2016.12.017>.
- 719 Debret, B., E. Albers, B. Walter, R. Price, J. D. Barnes, H. Beunon, S. Facq, D. P. Gillikin, N. Mattielli,
 720 and H. Williams (2019), Shallow forearc mantle dynamics and geochemistry: New insights from IODP
 721 Expedition 366, *Lithos*, 326-327, 230-245, doi:<https://doi.org/10.1016/j.lithos.2018.10.038>.
- 722 Deville, E., and A. Prinzhofer (2016), The origin of N₂-H₂-CH₄-rich natural gas seepages in ophiolitic
 723 context: A major and noble gases study of fluid seepages in New Caledonia, *Chemical Geology*, 440,
 724 139-147, doi:<https://doi.org/10.1016/j.chemgeo.2016.06.011>.
- 725 Dewandel, B., P. Lachassagne, F. Boudier, S. Al-Hattali, B. Ladouche, J. L. Pinault, and Z. Al-Suleimani
 726 (2005), A conceptual hydrogeological model of ophiolite hard-rock aquifers in Oman based on a
 727 multiscale and a multidisciplinary approach, *Hydrogeology Journal*, 13(5-6), 708-726,
 728 doi:10.1007/s10040-005-0449-2.
- 729 Donval, J. P., V. Guyader, and E. Boissy (2020), A simple method for the preparation and injection of
 730 gas mixtures into a gas chromatograph using a two-component device, *Journal of Chromatography A*,
 731 1631, 461579, doi:<https://doi.org/10.1016/j.chroma.2020.461579>.
- 732 Etiopie, G., M. Schoell, and H. Hosgormez (2011), Abiotic methane flux from the Chimaera seep and
 733 Tekirova ophiolites (Turkey): Understanding gas exhalation from low temperature serpentinization
 734 and implications for Mars, *Earth and Planetary Science Letters*, 310(1-2), 96-104,
 735 doi:10.1016/j.epsl.2011.08.001.
- 736 Etiopie, G., and B. Sherwood Lollar (2013), Abiotic methane on Earth, *Reviews of Geophysics*, 51(2),
 737 276-299, doi:10.1002/rog.20011.
- 738 Etiopie, G., B. Tsikouras, S. Kordella, E. Ifandi, D. Christodoulou, and G. Papatheodorou (2013),
 739 Methane flux and origin in the Othrys ophiolite hyperalkaline springs, Greece, *Chemical Geology*,
 740 347, 161-174, doi:<http://dx.doi.org/10.1016/j.chemgeo.2013.04.003>.
- 741 Etiopie, G., I. Vadillo, M. J. Whiticar, J. M. Marques, P. M. Carreira, I. Tiago, J. Benavente, P. Jiménez,
 742 and B. Urresti (2016), Abiotic methane seepage in the Ronda peridotite massif, southern Spain,
 743 *Applied Geochemistry*, 66, 101-113, doi:<http://dx.doi.org/10.1016/j.apgeochem.2015.12.001>.
- 744 Etiopie, G., and M. J. Whiticar (2019), Abiotic methane in continental ultramafic rock systems:
 745 Towards a genetic model, *Applied Geochemistry*, 102, 139-152,
 746 doi:<https://doi.org/10.1016/j.apgeochem.2019.01.012>.
- 747 Feth, J. H., S. M. Rogers, and C. E. Roberson (1961), Aqua de Ney, California, a spring of unique
 748 chemical character, *Geochimica et Cosmochimica Acta*, 22(2), 75-86,
 749 doi:[http://dx.doi.org/10.1016/0016-7037\(61\)90107-7](http://dx.doi.org/10.1016/0016-7037(61)90107-7).
- 750 Frouin, E., M. Bes, B. Ollivier, M. Quemeneur, A. Postec, D. Debroas, F. Armougom, and G. Erauso
 751 (2018), Diversity of Rare and Abundant Prokaryotic Phylotypes in the Prony Hydrothermal Field and
 752 Comparison with Other Serpentinite-Hosted Ecosystems, *Frontiers in Microbiology*, 9,
 753 doi:10.3389/fmicb.2018.00102.

- 754 Fryer, P., J. A. Pearce, and L. B. Stokking (1989), *Ocean Drilling Program Leg 125 preliminary report;*
 755 *Bonin/Mariana region*, 51 pp., Ocean Drilling Program, Texas A&M University, College Station, TX,
 756 United States.
- 757 Fryer, P., et al. (2020), Mariana serpentinite mud volcanism exhumes subducted seamount materials:
 758 implications for the origin of life, *Philosophical Transactions of the Royal Society A: Mathematical,*
 759 *Physical and Engineering Sciences*, 378(2165), 20180425, doi:doi:10.1098/rsta.2018.0425.
- 760 Fryer, P., C. G. Wheat, T. Williams, and t. E. Scientists (2018), Mariana Convergent Margin and South
 761 Chamorro Seamount., in *Proceedings of the International Ocean Discovery Program Volume 366*,
 762 edited, International Ocean Discovery Program, College Station TX, doi:10.14379/
 763 iodp.proc.366.2018.
- 764 Giampouras, M., C. J. Garrido, J. Zwicker, I. Vadillo, D. Smrzka, W. Bach, J. Peckmann, P. Jimenez, J.
 765 Benavente, and J. M. Garcia-Ruiz (2019), Geochemistry and mineralogy of serpentinization-driven
 766 hyperalkaline springs in the Ronda peridotites, *Lithos*, 350, 22, doi:10.1016/j.lithos.2019.105215.
- 767 Holm, N. G., C. Oze, O. Mousis, J. H. Waite, and A. Guilbert-Lepoutre (2015), Serpentinization and the
 768 Formation of H₂ and CH₄ on Celestial Bodies (Planets, Moons, Comets), *Astrobiology*, 15(7), 587-600,
 769 doi:10.1089/ast.2014.1188.
- 770 Hulme, S. M., C. G. Wheat, P. Fryer, and M. J. Mottl (2010), Pore water chemistry of the Mariana
 771 serpentinite mud volcanoes: A window to the seismogenic zone, *Geochemistry Geophysics*
 772 *Geosystems*, 11.
- 773 Kelemen, P. B., and J. Matter (2008), In situ carbonation of peridotite for CO₂ storage, *Proceedings of*
 774 *the National Academy of Sciences of the United States of America*, 105(45), 17295-17300.
- 775 Kelemen, P. B., J. Matter, E. E. Streit, J. F. Rudge, W. B. Curry, and J. Blusztajn (2011), Rates and
 776 Mechanisms of Mineral Carbonation in Peridotite: Natural Processes and Recipes for Enhanced, in
 777 situ CO₂ Capture and Storage, in *Annual Review of Earth and Planetary Sciences*, Vol 39, edited by R.
 778 Jeanloz and K. H. Freeman, pp. 545-576, doi:10.1146/annurev-earth-092010-152509.
- 779 Kelley, D. S., et al. (2001), An off-axis hydrothermal vent field near the Mid-Atlantic Ridge at 30
 780 degrees N, *Nature*, 412(6843), 145-149.
- 781 Kelley, D. S., et al. (2005), A serpentinite-hosted ecosystem: The lost city hydrothermal field, *Science*,
 782 307(5714), 1428-1434.
- 783 Khoury, H. N., E. Salameh, I. D. Clark, P. Fritz, W. Bajjali, A. E. Milodowski, M. R. Cave, and W. R.
 784 Alexander (1992), A natural analogue of high pH cement pore waters from the Maqarin area of
 785 northern Jordan. I: introduction to the site, *Journal of Geochemical Exploration*, 46(1), 117-132,
 786 doi:[https://doi.org/10.1016/0375-6742\(92\)90103-F](https://doi.org/10.1016/0375-6742(92)90103-F).
- 787 Kraus, E. A., D. Nothaft, B. W. Stamps, K. R. Rempfert, E. T. Ellison, J. M. Matter, A. S. Templeton, E. S.
 788 Boyd, and J. R. Spear (2020), Molecular evidence for an active microbial methane cycle in subsurface
 789 serpentinite-hosted groundwaters in the Samail Ophiolite, Oman, *Applied and Environmental*
 790 *Microbiology*, AEM.02068-02020, doi:10.1128/AEM.02068-20.
- 791 Launay, J., and J. C. Fontes (1985), Les sources thermales de Prony (Nouvelle Calédonie) et leurs
 792 précipités chimiques. exemple de formation de brucite primaire., *Geologie de la France*, 1, 83-100.
- 793 Leleu, T., V. Chavagnac, A. Delacour, C. Noiriel, G. Ceuleneer, M. Aretz, C. Rommevaux, and S.
 794 Ventalon (2016), TRAVERTINES ASSOCIATED WITH HYPERALKALINE SPRINGS: EVALUATION AS A
 795 PROXY FOR PALEOENVIRONMENTAL CONDITIONS AND SEQUESTRATION OF ATMOSPHERIC CO₂,
 796 *Journal of Sedimentary Research*, 86(11), 1328-1343, doi:10.2110/jsr.2016.79.
- 797 Leong, J. A. M., and E. L. Shock (2020), Thermodynamic constraints on the geochemistry of low-
 798 temperature, continental, serpentinization-generated fluids, *American Journal of Science*, 320(3),
 799 185-235, doi:10.2475/03.2020.01.
- 800 Ligi, M., E. Bonatti, M. Cuffaro, and D. Brunelli (2013), Post-Mesozoic Rapid Increase of Seawater
 801 Mg/Ca due to Enhanced Mantle-Seawater Interaction, *Scientific Reports*, 3, doi:10.1038/srep02752.
- 802 Lods, G., D. Roubinet, J. M. Matter, R. Leprovost, P. Gouze, and T. Oman Drilling Project Sci (2020),
 803 Groundwater flow characterization of an ophiolitic hard-rock aquifer from cross-borehole multi-level
 804 hydraulic experiments, *J. Hydrol.*, 589, 18, doi:10.1016/j.jhydrol.2020.125152.

- 805 Marques, J. M., P. M. Carreira, M. R. Carvalho, M. J. Matias, F. E. Goff, M. J. Basto, R. C. Graça, L.
806 Aires-Barros, and L. Rocha (2008), Origins of high pH mineral waters from ultramafic rocks, Central
807 Portugal, *Applied Geochemistry*, 23(12), 3278-3289.
- 808 Marques, J. M., G. Etiope, M. O. Neves, P. M. Carreira, C. Rocha, S. D. Vance, L. Christensen, A. Z.
809 Miller, and S. Suzuki (2018), Linking serpentinization, hyperalkaline mineral waters and abiotic
810 methane production in continental peridotites: an integrated hydrogeological-bio-geochemical
811 model from the Cabeço de Vide CH₄-rich aquifer (Portugal), *Applied Geochemistry*, 96, 287-301,
812 doi:<https://doi.org/10.1016/j.apgeochem.2018.07.011>.
- 813 Maurizot, P., B. Sevin, S. Lesimple, J. Collot, J. Jeanpert, B. Robineau, M. Patriat, S. Etienne, and C.
814 Monnin (2020), Mineral resources and prospectivity of non-ultramafic rocks of New-Caledonia, in
815 *New Caledonia: Geology, Geodynamic Evolution and Mineral Resources*, edited by N. Mortimer, pp.
816 215-245, Geological Society London, London, doi:<https://doi.org/10.1144/M51-2016-9>.
- 817 Mei, N., A. Postec, C. Monnin, B. Pelletier, C. E. Payri, B. Ménez, E. Frouin, B. Ollivier, G. Erauso, and
818 M. Quéménéur (2016), Metagenomic and PCR-Based Diversity Surveys of [FeFe]-Hydrogenases
819 Combined with Isolation of Alkaliphilic Hydrogen-Producing Bacteria from the Serpentinite-Hosted
820 Prony Hydrothermal Field, New Caledonia, *Frontiers in Microbiology*, 7(1301),
821 doi:10.3389/fmicb.2016.01301.
- 822 Menez, B. (2020), Abiotic Hydrogen and Methane: Fuels for Life, *Elements*, 16(1), 39-46,
823 doi:10.2138/gselements.16.1.39.
- 824 Menez, B., V. Pasini, and D. Brunelli (2012), Life in the hydrated suboceanic mantle, *Nature*
825 *Geoscience*, 5(2), 133-137, doi:10.1038/ngeo1359.
- 826 Meyer-Dombard, D. R., K. M. Woycheese, E. N. Yargicoglu, D. Cardace, E. L. Shock, Y. Gulecal-Pektas,
827 and M. Temel (2015), High pH microbial ecosystems in a newly discovered, ephemeral, serpentinizing
828 fluid seep at Yanartas (Chimera), Turkey, *Frontiers in Microbiology*, 5, doi:10.3389/fmicb.2014.00723.
- 829 Milkov, A. V., and G. Etiope (2018), Revised genetic diagrams for natural gases based on a global
830 dataset of >20,000 samples, *Organic Geochemistry*, 125, 109-120,
831 doi:<https://doi.org/10.1016/j.orggeochem.2018.09.002>.
- 832 Miller, H. M., J. M. Matter, P. Kelemen, E. T. Ellison, M. E. Conrad, N. Fierer, T. Ruchala, M. Tominaga,
833 and A. S. Templeton (2016), Modern water/rock reactions in Oman hyperalkaline peridotite aquifers
834 and implications for microbial habitability, *Geochimica et Cosmochimica Acta*, 179, 217-241,
835 doi:<http://dx.doi.org/10.1016/j.gca.2016.01.033>.
- 836 Monnin, C., et al. (2014), Fluid chemistry of the low temperature hyperalkaline hydrothermal system
837 of Prony Bay (New Caledonia), *Biogeosciences*, 11(20), 5687-5706, doi:10.5194/bg-11-5687-2014.
- 838 Monnin, C., J. Tamborski, S. Bejannin, M. Souhaut, M. Rogues, P. Olivier, and P. van Beek (2019),
839 Freshening of a Coastal Karst Aquifer Revealed by the Temporal Changes in a Spring Water
840 Composition (La Palme, Southern France), *Hydrology*, 6(2), 17, doi:10.3390/hydrology6020045.
- 841 Morrill, P. L., J. G. Kuenen, O. J. Johnson, S. Suzuki, A. Rietze, A. L. Sessions, M. L. Fogel, and K. H.
842 Nealson (2013), Geochemistry and geobiology of a present-day serpentinization site in California: The
843 Cedars, *Geochimica Et Cosmochimica Acta*, 109, 222-240, doi:10.1016/j.gca.2013.01.043.
- 844 Mottl, M. J., C. G. Wheat, P. Fryer, J. Gharib, and J. B. Martin (2004), Chemistry of springs across the
845 Mariana forearc shows progressive devolatilization of the subducting plate, *Geochimica Et*
846 *Cosmochimica Acta*, 68(23), 4915-4933.
- 847 Myagkiy, A., I. Moretti, and F. Brunet (2020), Space and time distribution of subsurface
848 H₂concentration in so-called "fairy circles": Insight from a conceptual 2-D transport model, *BSGF -*
849 *Earth Sciences Bulletin*, 191, doi:10.1051/bsgf/2020010.
- 850 Neal, C., and P. Shand (2002), Spring and surface water quality of the Cyprus ophiolites, *Hydrology*
851 *and Earth System Sciences*, 6(5), 797-817.
- 852 Neal, C., and G. Stanger (1983), Hydrogen generation from mantle source rocks in Oman, *Earth and*
853 *Planetary Science Letters*, 66, 315-320.
- 854 Paukert, A. N., J. M. Matter, P. B. Kelemen, E. L. Shock, and J. R. Havig (2012), Reaction path modeling
855 of enhanced in situ CO₂ mineralization for carbon sequestration in the peridotite of the Samail

- 856 Ophiolite, Sultanate of Oman, *Chemical Geology*, 330–331(0), 86-100,
 857 doi:10.1016/j.chemgeo.2012.08.013.
- 858 Pelletier, B., C. Chevillon, J. L. Menou, J. Butscher, E. Folcher, C. Geoffray, J. M. Bore, and J. Perrier
 859 (2006), Plongées, forage et cartographie Baie du Prony et Banc Gail, lagon Sud de Nouvelle-
 860 Calédonie, campagne 2005-NC-PL du N.O. ALIS, 13-17 juin 2005 et cartographie baie du Prony N.O.
 861 ALIS, 25-26 septembre 2005. Rapports de missions, , *Sci. Terre, Geol-Geophys.*, 70, 44.
- 862 Pelletier, B., et al. (2011), Campagne HYDROPRONY du N.O. ALIS, 28 octobre – 13 novembre 2011.
 863 Rapport de mission IRD Nouméa. *Rep.*, 41 pp.
- 864 Plank, T., and C. E. Manning (2019), Subducting carbon, *Nature*, 574(7778), 343-352,
 865 doi:10.1038/s41586-019-1643-z.
- 866 Postec, A., et al. (2015), Microbial diversity in a submarine carbonate edifice from the serpentinizing
 867 hydrothermal system of the Prony Bay (New Caledonia) over 6-year period, *Frontiers in Microbiology*,
 868 doi:<http://dx.doi.org/10.3389/fmicb.2015.00857>.
- 869 Price, R., E. S. Boyd, T. M. Hoehler, L. M. Wehrmann, E. Bogason, H. P. Valtýsson, J. Örlygsson, B.
 870 Gautason, and J. P. Amend (2017), Alkaline vents and steep Na⁺ gradients from ridge-flank basalts—
 871 Implications for the origin and evolution of life, *Geology*, 45(12), 1135-1138, doi:10.1130/G39474.1.
- 872 Quemeneur, M., et al. (2014), Spatial distribution of microbial communities in the shallow submarine
 873 alkaline hydrothermal field of the Prony Bay, New Caledonia, *Environmental Microbiology Reports*,
 874 6(6), 665-674, doi:10.1111/1758-2229.12184.
- 875 Quémeneur, M., G. Erauso, M. Bartoli, C. Vandecasteele, L. Wils, L. Gil, C. Monnin, B. Pelletier, and A.
 876 Postec (2021), *Alkalicella caledoniensis* gen. nov., sp. nov., a novel alkaliphilic anaerobic bacterium
 877 isolated from ‘La Crouen’ alkaline thermal spring, New Caledonia., *International Journal of Systematic
 878 and Evolutionary Microbiology*, 71, doi:10.1099/ijsem.0.004810.
- 879 Quémeneur, M., A. Palvadeau, A. Postec, C. Monnin, V. Chavagnac, B. Ollivier, and G. Erauso (2015),
 880 Endolithic microbial communities in carbonate precipitates from serpentinite-hosted hyperalkaline
 881 springs of the Voltri Massif (Ligurian Alps, Northern Italy), *Environ Sci Pollut Res*, 1-12,
 882 doi:10.1007/s11356-015-4113-7.
- 883 Reeves, E. P., and J. Fiebig (2020), Abiotic Synthesis of Methane and Organic-Compounds in Earth's
 884 Lithosphere, *Elements*, 16(1), 25-31, doi:10.2138/gselements.16.1.25.
- 885 Rempfert, K. R., H. M. Miller, N. Bompard, D. Nothaft, J. M. Matter, P. Kelemen, N. Fierer, and A. S.
 886 Templeton (2017), Geological and Geochemical Controls on Subsurface Microbial Life in the Samail
 887 Ophiolite, Oman, *Frontiers in Microbiology*, 8(56), doi:10.3389/fmicb.2017.00056.
- 888 Sader, J. A., M. I. Leybourne, B. McClenaghan, and M. S. Hamilton (2007), Low-temperature
 889 serpentinization processes and kimberlite groundwater signatures in the Kirkland Lake and Lake
 890 Timiskiming kimberlite fields, Ontario, Canada: implications for diamond exploration, *Geochemistry:
 891 Exploration, Environment, Analysis*, 7, 3-21.
- 892 Sano, Y., A. Urabe, H. Wakita, and H. Wushiki (1993), Origin of hydrogen-nitrogen gas seeps, Oman,
 893 *Applied Geochemistry*, 8(1), 1-8, doi:[https://doi.org/10.1016/0883-2927\(93\)90053-J](https://doi.org/10.1016/0883-2927(93)90053-J).
- 894 Schrenk, M. O., W. J. Brazelton, and S. Q. Lang (2013), Serpentinization, Carbon, and Deep Life, in
 895 *Carbon in Earth*, edited by R. M. Hazen, A. P. Jones and J. A. Baross, pp. 575-606,
 896 doi:10.2138/rmg.2013.75.18.
- 897 Sciarra, A., A. Saroni, G. Etiope, M. Coltorti, F. Mazzarini, C. Lott, F. Grassa, and F. Italiano (2019),
 898 Shallow submarine seep of abiotic methane from serpentinized peridotite off the Island of Elba, Italy,
 899 *Applied Geochemistry*, 100, 1-7, doi:<https://doi.org/10.1016/j.apgeochem.2018.10.025>.
- 900 Seyfried Jr, W. E., N. J. Pester, B. M. Tutolo, and K. Ding (2015), The Lost City hydrothermal system:
 901 Constraints imposed by vent fluid chemistry and reaction path models on subseafloor heat and mass
 902 transfer processes, *Geochimica et Cosmochimica Acta*, 163(0), 59-79,
 903 doi:<http://dx.doi.org/10.1016/j.gca.2015.04.040>.
- 904 Sissmann, O., et al. (2019), Abiogenic formation of H₂, light hydrocarbons and other short-chain
 905 organic compounds within the serpentinite mud volcanoes of the Marianna Trench, *E3S Web Conf.*,
 906 98, 02011.
- 907 Stanger, G. (1985), *The hydrogeology of the Oman mountains.*, The Open University, UK.

- 908 Suzuki, S., S. Ishii, A. Wu, A. Cheung, A. Tenney, G. Wanger, J. G. Kuenen, and K. H. Nealson (2013),
909 Microbial diversity in The Cedars, an ultrabasic, ultrareducing, and low salinity serpentizing
910 ecosystem, *Proceedings of the National Academy of Sciences of the United States of America*,
911 *110*(38), 15336-15341, doi:10.1073/pnas.1302426110.
- 912 Szponar, N., W. J. Brazelton, M. O. Schrenk, D. M. Bower, A. Steele, and P. L. Morrill (2012),
913 Geochemistry of a continental site of serpentization, the Tablelands Ophiolite, Gros Morne
914 National Park: A Mars analogue, *Icarus*, *224*(2), 286-296, doi:10.1016/j.icarus.2012.07.004.
- 915 Truche, L., T. M. McCollom, and I. Martinez (2020), Hydrogen and Abiotic Hydrocarbons: Molecules
916 that Change the World, *Elements*, *16*(1), 13-18.
- 917 Vacquand, C., E. Deville, V. Beaumont, F. Guyot, O. Sissmann, D. Pillot, C. Arcilla, and A. Prinzhofer
918 (2018), Reduced gas seepages in ophiolitic complexes: Evidences for multiple origins of the H₂-CH₄-
919 N₂ gas mixtures, *Geochimica et Cosmochimica Acta*, *223*, 437-461,
920 doi:<https://doi.org/10.1016/j.gca.2017.12.018>.
- 921 Young, C., J. B. Martin, J. Branyon, A. Pain, A. Valle-Levinson, I. Marino-Tapia, and M. R. Vieyra (2018),
922 Effects of short-term variations in sea level on dissolved oxygen in a coastal karst aquifer, Quintana
923 Roo, Mexico, *Limnology and Oceanography*, *63*(1), 352-362, doi:10.1002/lno.10635.
- 924 Yuce, G., et al. (2014), Origin and interactions of fluids circulating over the Amik Basin (Hatay, Turkey)
925 and relationships with the hydrologic, geologic and tectonic settings, *Chemical Geology*, *388*, 23-39,
926 doi:<http://dx.doi.org/10.1016/j.chemgeo.2014.09.006>.
- 927 Zgonnik, V., V. Beaumont, N. Larin, D. Pillot, and E. Deville (2019), Diffused flow of molecular
928 hydrogen through the Western Hajar mountains, Northern Oman, *Arab. J. Geosci.*, *12*(3), 10,
929 doi:10.1007/s12517-019-4242-2.

930